SPROUTING ANGIOGENESIS DURING RETINAL DEVELOPMENT AND WOUND HEALING

Diana Cristina Chong

A dissertation submitted to the faculty at the University of North Carolina at Chapel Hill in partial fulfillment of the requirements for the degree of Doctor of Philosophy in the Curriculum of Genetics and Molecular Biology.

Chapel Hill
2017

Approved By:

Victoria Bautch

Kathleen Caron

Frank Conlon

John Rawls

Paul Dayton

ABSTRACT

Diana Cristina Chong: Sprouting Angiogenesis During Retinal Development and Wound Healing
(Under the direction of Victoria Bautch)

Endothelial cells, the cells that line blood vessels, become activated during development to sprout and form new vessels in a process termed angiogenesis. During development, sprouting angiogenesis is robust and is the main driving force behind vascularization of new tissues in the embryo. In contrast, endothelial cells are mainly quiescent in the adult and only become reactivated during physiological or pathological angiogenesis. The bone morphogenetic protein (BMP) pathway has been shown to be a pro-angiogenic cue. During postnatal retinal development, BMP receptors are expressed in the retinal vasculature and BMP ligands are expressed throughout the retina. Here, we show that deletion of BMP receptors, Alk1, Alk2, Alk3, and BMPR2 affect sprouting angiogenesis during development. Endothelial specific deletion of Alk2, Alk3, and BMPR2 resulted in decreased sprouting at the vascular front as well as branching in the vascular plexus, whereas deletion of Alk1 resulted in increased sprouting. These data point to a requirement of BMP signaling for proper patterning of the retinal vasculature during development. We also analyzed tortuous microvessels, abnormal vessels that arise during the wound healing process. Tortuous vessels are observed in many diseases, most notably cancer and diabetes. However, the causes and consequences of these abnormal vessels have not been elucidated. Here, we use intravital, high-resolution imaging to examine the formation, resolution, and sprouting of tortuous

microvessels during wound healing. We found that tortuous microvessels are mainly located 100-300 μm from the wound center and that tortuous microvessels resolved by becoming normal again. Additionally, using fluorescent, microcarrier beads we found that beads became stuck in tortuous microvessels suggesting differences in flow. The shapes of endothelial cells within tortuous microvessels are round, indicative of activated cells, and exhibit sprout initiations at a higher frequency than normal vessels. Thus, we highlight an important, undiscovered feature of tortuous microvessels, sprouting, that can be used as a therapeutic target to normalize tortuous vessels during disease.

I dedicate this work to my family and friends, especially Cody and Maya.

ACKNOWLEDGEMENTS

There are many people I'd like to thank that have helped me reach this point. First, I would like to thank my committee members, Drs. Kathleen Caron, Frank Conlon, John Rawls, and Paul Dayton. They have offered me lots of support and guidance throughout grad school and helped me develop my story. I would especially like to thank my mentor, Dr. Victoria Bautch. Being in her lab has made me a critical thinker and a stronger mentor. I appreciate the time and effort she put into making me a better scientist. I would also like to thank my previous mentor, Dr. Ondine Cleaver at UTSW. She introduced me to blood vessels and development, taught me embryology dissection, and encouraged me to go to graduate school.

I would also like to thank members of the Bautch lab, both past and present. Dr. David Wiley was my first mentor in the lab and he patiently taught me how to handle zebrafish. Drs. John Chappell, Erich Kushner, Sophie Dalpra, John Pelton, and Catherine Wright were in the lab when I first joined and Drs. Kevin Mouillesseaux, Joshua Boucher, Jessica Nesmith, Zhixian Yu, and Dana Ruter joined at the same time or after me. I still remain in close contact with most of these people, even though most of them have moved away. I received help with grants, presentations, grad school life, post grad school advice from everyone, and I thank all of you for helping me. There are also numerous lab managers and undergrads (too many to name), but I want to acknowledge Jess Heinz, Kelsey Harvey, Elle Law, Michael Zheng, Hong Lee, Theresa Nguyen, and Katy Citrin for helping me

maintain my mouse colony. Everyone contributed to the great lab atmosphere and made it a great place to work. I specifically want to thank Lyndsay Wylie. She challenges me scientifically and personally, and it's been incredible seeing her become an amazing scientist. She also gives me lots of mommy advice and sets a great example on how to balance family and work.

I want to thank all of my friends, both in and out of grad school. Joy, Jenny H., Leslie, Kelsey G., Mike, Joe, Alex, Becky, Dan, Hailey, Jenny M., Samira, Aly, Ye Lin, Chris, Laura, Lin, and many more. You guys have helped me view my research from a different point of view, but more importantly you have helped me unwind and have fun in grad school.

My family in Dallas has been very supportive. My mother always has encouraging words to say in the toughest of times. She gives me the drive to be stronger and better.

Lastly, I want to thank my partner Cody and our daughter Maya. Cody dropped everything to come to NC with me and help me pursue my dream. He encourages me when I'm writing late at night and he has no doubt that I will succeed. As a non-scientist, he also keeps me sane and gives me real world perspective. Maya is a new addition, and although she can't speak yet, I know she believes in me. I strive to set a good, female, leadership example for her, and she makes me stronger for it.

TABLE OF CONTENTS

LIST OF FIGURES

LIST OF ABBREVIATIONS

ACVR1	Activin receptor type-1
BAMBI	BMP and activin membrane bound inhibitor
BMP	Bone morphogenetic protein
BMPR2	Bone morphogenetic protein type II Receptor
BRE	BMP response element
DPW	Days post wounding
E	Embryonic day
ECM	Extracellular matrix
FGF	Fibroblast growth factor
GFP	Green fluorescent protein
HUVEC	Human umbilical venous endothelial cells
HAEC	Human aortic endothelial cells
ICAM-1	Intercellular adhesion molecule 1
iECKO	Inducible endothelial cell knock out
MAPK	Mitogen-activated protein kinase
MLEC	Mouse lung endothelial cells
MYOX	Myosin X
PECAM	Platelet endothelial cell adhesion molecule
PDGF	Platelet-derived growth factor
PGF	Placental growth factor
TI	Tortuosity index
TGF-β	Transforming growth factor β

VCAM-1	Vascular cell adhesion molecule 1
VEGF	Vascular endothelial growth factor
VEGF-R	Vascular endothelial growth factor receptor

Chapter 1: General Introduction

1.1 Sprouting angiogenesis

My research projects have focused on sprouting angiogenesis and how sprouting is affected in different vascular beds in normal and mutant backgrounds. This section describes the processes involved in blood vessel development and signaling pathways that are major contributors.

Blood Vessel Formation: vasculogenesis and angiogenesis

The circulatory system is the first functional organ system established in the vertebrate embryo, and it consists of blood vessels which transport nutrients and oxygen to tissues and provide conduits for waste removal [1-3] . Blood vessels are formed through two main processes: *vasculogenesis* and *angiogenesis*. Angioblasts, derived from mesoderm cells, differentiate into endothelial cells, the cells that line blood vessels, starting at embryonic day (E) 7.5. During this time, angioblasts fuse and coalesce to form blood vessel tubes in a process termed *vasculogenesis* [4]. The tubes become arranged in a primitive vascular plexus that subsequently grow into a complex hierarchy of blood vessels, including arteries, veins, and capillaries, through a process termed *angiogenesis* [5]. Angiogenesis is the formation of new blood vessels from pre-existing vessels, and can occur through vessel sprouting, remodeling, pruning, or intussusception [5, 6]. This chapter will focus on sprouting angiogenesis which is defined as an endothelial cell budding from its parent vessel to initiate

a new vessel. The mechanisms and processes involved in sprouting will be described in detail in the following section.

Signaling pathways regulating angiogenesis

One of the main signaling pathways that regulates vasculogenesis and angiogenesis is the vascular endothelial growth factor-A (VEGF) pathway. VEGF-A is a secreted cytokine and plays a role in endothelial cell differentiation, proliferation, migration, survival, vessel permeability, and sprouting [7, 8]. Genetic loss of only one copy of the *VegfA* gene leads to embryonic lethality at an early stage (between E8.5-E9.5) [9], highlighting the importance of this signaling pathway during development. Since the discovery of VEGF and its critical role in angiogenesis, other pathways that also regulate sprouting angiogenesis have emerged, such as BMP, Wnt, and Notch pathways [10-12].

Sprouting angiogenesis, the main driving force increasing vessel density, initiates when endothelial cells receive extracellular stimuli and guidance cues that alter intracellular cytoskeletal dynamics and polarity to initiate outward migration from the parent vessel and become tip cells, the leading cells of sprouts [13-15]. The endothelial cells that trail behind the tip cells are termed "stalk" cells [11, 14]. Stalk cells are primarily involved in sprout elongation and lumen formation. Differences in protein expression between neighboring endothelial cells establish the heterogeneity essential for tip/stalk cell selection and activation of downstream signaling components [16, 17]. Molecular signatures for both tip and stalk cells have been identified, most notably in the Notch and VEGF pathways [11, 18]. Tip cells have increased VEGF Receptor 2 (VEGFR-2) and Delta-like 4 (Dll4) signaling, while stalk cells have increased Notch and VEGF Receptor 1 (VEGFR-1) signaling [11]. However, the

crosstalk between these and other pathways have led to a more complex regulatory network that includes feedback loops and receptor stability [19-22]. BMP signaling also impacts sprouting angiogenesis and will be discussed in a later section.

1.1 Angiogenesis during development, physiological and pathological conditions

I have examined blood vessel growth during development and in adults. In this section, I highlight the similarities and differences between angiogenesis in embryos, adults, and during disease.

Developmental angiogenesis

During embryonic development, sprouting angiogenesis increases the vascular network. This expansion perfuses the embryo with blood vessels to provide the essential nutrients and oxygen required for proper growth. Because blood vessels are a critical component for development, perturbations in the pathways that regulate angiogenesis lead to embryonic lethality. For example, global deletion of any of the VEGF receptors (*Vegfr-1,2,3*) which bind VEGF ligands leads to embryonic lethality between E8.5-E12.5 [23]. The phenotypes associated with deletion of each receptor can vary as they each have different roles in the pathway. $Vegfr1^{-/-}$ embryos have excessive endothelial proliferation and lumen obstruction [24, 25], $Vegfr2^{-/-}$ embryos have deficient endothelial cell differentiation and lack blood vessels [26], and $Vegfr3^{-/-}$ embryos have vascular remodeling defects and pericardial fluid accumulation [27]. To add another level of complexity, the VEGF receptors can also form heterodimers with each other, as well as other co-receptors, such as neuropilins [23]. Although I have only described the VEGF-A pathway in short, there are many more

signaling pathways that contribute to developmental angiogenesis [5, 6, 12, 14].

Additionally, crosstalk between multiple pathways is critical for proper vessel patterning of

the embryo.

Physiological angiogenesis

During physiological angiogenesis, some of the similar pathways that drive

developmental angiogenesis are still present, such as VEGF-A. However, a significant

difference between developmental and physiological angiogenesis is the infiltration of

inflammatory cells, such as neutrophils and macrophages, that secrete growth factors to

recruit and generate new blood vessels during physiological angiogenesis [28].

Most vascular endothelial cells in adults are non-mitogenic and quiescent [5]. Yet,

endothelial cells are activated in adults during physiological and pathological angiogenesis.

Physiological angiogenesis refers to natural processes in which blood vessels are required to

aid in tissue turnover, such as wound healing or menstruation, or provide enhanced

enrichment, such as pregnancy [28]. During physiological angiogenesis, growth factors, such

as VEGF-A, placental growth factor (PGF), and fibroblast growth factor (FGF), become

secreted to activate endothelial cells to migrate, sprout, and form new vessels in a process

termed *neovascularization* [28, 29]. However, after the new tissue is healed or pregnancy is

complete, the newly formed blood vessels are no longer necessary and apoptosis of

endothelial cells occurs to prune the vascular network as well as cessation of growth factor

secretion to prevent new vessels from forming [30, 31]. In this manner, physiological

angiogenesis has a built-in "shut-off switch" that allows tissues, and blood vessels, to resolve

over time.

Pathological angiogenesis

Pathological angiogenesis is the growth of new blood vessels associated with disease. Pathological angiogenesis shares many characteristics with developmental and physiological angiogenesis, such as inflammation and increased growth factor and cytokine signaling [28]. However, during pathological angiogenesis, pro-angiogenic signaling mechanisms persist, leading to disordered endothelial cells and/or an increased vascular network [28]. Pathological angiogenesis can aid diseases in many ways. For instance, tumor cells secrete growth factors and cytokines to activate pro-angiogenic pathways and recruit vessels. Blood vessels then aid tumors by 1) increasing nutrient and oxygen delivery to the tumor, allowing the tumor to grow rapidly and 2) providing more avenues for tumor cells to intravasate into the vessels and metastasize at new sites [32, 33]. Since pathological angiogenesis activates similar pathways to physiological angiogenesis, it is difficult to tease apart therapeutic interventions that will only affect pathogenesis without interfering with normal, healing, biological processes.

1.2 Wound Healing

I examine physiological angiogenesis in a wound healing model. Here, I describe the properties of wound healing and what is known about angiogenesis during wound healing.

Wound healing demographics and mechanism

Over thirty-five million cutaneous wounds that require medical intervention occur annually in US [34]. Of those, an estimated two to five million result in chronic wounds, or

wounds that persist. Patients with diabetes are a higher risk for developing chronic wounds, mainly manifesting as foot ulcers that can lead to amputation [35, 36]. The financial costs associated with treatment of chronic wounds is high, estimated at $45,000 per patient for diabetic foot ulcers alone [37]. Thus, better treatments or faster healing rates of wounds is essential for better quality of life and decreased financial burden.

Wound healing occurs in three main phases: inflammatory, proliferative, and remodeling [30, 38, 39]. The inflammatory phase is initiated immediately after a wound is made. During this phase, fibroblasts and polymorphonuclear cells invade the wound site and secrete growth factors promoting vessel growth and remodeling [30, 40]. Fibroblasts also deposit extracellular matrix (ECM) to support subsequent cellular influx and angiogenic growth [38]. In the proliferative phase, angiogenesis occurs in response to secreted growth factors from macrophages and keratinocytes to facilitate nutrient delivery to the wound site [37]. Proliferation of endothelial cells at this stage is critical, as vessels are the main conduits for transport of immune cells and nutrients to the wound, and wounds are not able to heal properly without sufficient vasculature [41]. In the remodeling phase, the wound has finished healing and the programs that became active in the previous phases are turned off. During this phase, the wound contracts, angiogenesis ceases, apoptosis of various cell types, (including endothelial cells) occurs, and a scar is formed where the tissue was once broken [30].

Angiogenesis during wound healing

Neovascularization is robustly activated during wound healing and new vessels are mainly formed through angiogenesis. The inflammatory response initiated by tissue injury

stimulates macrophages and keratinocytes to produce high levels of VEGF [42]. Moreover, VEGF is produced in response to hypoxia at the wound site [43]. In addition to VEGF, fibroblast growth factor -2 (FGF-2), platelet-derived growth factor (PDGF), TGF-β ligands, BMP ligands and more are secreted to promote angiogenesis [44]. The influx of pro-angiogenic factors stimulates capillaries to grow rapidly, filling the wound with a vascular network that can be up to ten times more dense than normal tissue [43]. Notably, most of the newly formed vessels are immature, leaky, and nonfunctional [45]. After the proliferative phase, the vascular network is pruned back to normal levels. Failure of vascular pruning can lead to increased scarring and decreased strength in the newly generated tissue [45].

In chronic, nonhealing wounds, inflammation persists and there is a delay or no progression to the remodeling phase [45]. Chronic wounds show a decrease in angiogenesis and overall less vessels in the regenerated tissue. Studies in which ischemia is induced in Type 2 diabetic mice show that diabetic wounds have delayed wound healing rates due to persistent inflammation [46] and decreased angiogenesis [47]. Decreased vascular networks in wounded tissue can lead to necrosis and limb amputation in extreme cases [48, 49]. On the other hand, increasing angiogenesis at the wound site accelerates the rate of wound healing [50, 51]. For this reason, current wound healing therapies are focused on increasing vessel density near the wound. One example consists of building vascularized scaffolds that can biodegrade once transplanted into wounded tissue [41] or scaffolds that are embedded with growth factors to attract more blood vessels [52]. Yet, other studies are focused on the potential of stem cells to jumpstart endothelial differentiation and increase vessel formation at the wound [46, 53]. Since increasing angiogenesis at the would correlates to accelerated

wound healing [50], understanding mechanisms that increase vessel density at the wound site are of great interest.

1.3 Tortuous Vessels

My thesis project uncovered a previously unknown characteristic of tortuous vessels, sprouting, that I observed during wound healing. Here, I describe what is known about tortuous vessels and what diseases are associated with formation of tortuous vessels.

Tortuous vessel morphologies and characteristics

Tortuous vessels are abnormal vessels characterized as having oscillating S curves, kinking/bending, looping, or a spiral twisting morphology (**Figure 1.1**) [54]. Although these vessels have been observed for decades in many diseases and in wounds, the mechanisms correlated to the causes and consequences of tortuous vessels remain poorly understood. Part of the difficulty in studying tortuous vessels is that these vessel types have only been observed *in vivo*, making it challenging to unravel the complex signaling mechanisms using genetic tools. Clinical observations have linked tortuous vessels with wounds, aging, atherosclerosis, hypertension, genetic defects and diabetes, and are many times used as a prognostic biomarker for these diseases [54]. Tortuous vessels have decreased or abnormal endothelial cell junctions [55] and as a consequence, are leaky and permeable [56]. Of note, innate tortuous vessels exist, such as collateral vessels, that do not share characteristics with disease-associated tortuosity aside from their distinct morphologies [57]. Thus, the information provided in this section focuses on tortuous vessels that arise from pathogenesis or wound healing.

Causes of tortuous vessel formation

Although the mechanisms involved in tortuous vessel formation have not been elucidated, some implicated factors include: 1) biomechanical forces, such as an increase in blood pressure [58], 2) reduced axial tension due to vessel elongation [59], 3) weakening of the arterial wall or surrounding extracellular matrix [60, 61], and 4) an influx of growth factor and cytokine secretion [62-64]. Additional studies have hypothesized mechanical instability and remodeling as one of the mechanisms for initiation and development of tortuous vessels [54, 65, 66].

Changes in mechanical forces, induced by blood flow, leads to altered endothelial cell gene expression. Computational models predict that curved vessels experience increased shear stress on the outer curvature [67] and that S-curved vessels experience disturbed flow that is positively correlated to vessel diameter [68]. Genes associated with inflammation, such as vascular cell adhesion molecule 1 (VCAM-1), are upregulated by endothelial cells experiencing disturbed flow [69]. Furthermore, studies using microarrays performed in human aortic endothelial cells (HAEC) reveal a subset of genes that are differentially expressed under laminar and disturbed flow conditions [70]. This differential activation of downstream signaling components leads to endothelial cell heterogeneity between cells in normal and tortuous vessels.

One of the signaling events that is compromised is the crosstalk between tortuous endothelial cells and smooth muscle cells. Disturbed flow activates signals that instruct smooth muscle cells to relax [71] which in turn activates proliferation of endothelial cells within tortuous vessels [72, 73]. The increase in proliferation is confined to a vessel segment

that is connected to other vessels at both endpoints. Because the vessel segment is not able to extend and is experiencing increased rates of cell division, it will buckle and take on the hallmark appearance of tortuosity [54]. Additionally, alterations in the ECM can induce tortuous vessel formation. Pietramaggiori et al. showed that applying a continuous tensile strength of 0.50 Newtons to the rat ear, induced matrix changes and caused vessels to become tortuous [74]. Genetically, tortuous vessel formation has been linked to overexpression of the growth factors VEGF-A [75, 76] and VEGF-C [63], loss of the transcription factor *Elk3* [77], and deletion of the ECM component *Fibulin5* [61].

Tortuous vessels during wound healing

Tortuous vessels have been observed during wound healing by use of dye injection [66] and Doppler imaging or laser speckling which uses blood flow to visualize blood vessels [78, 79]. During wound healing, the number of tortuous vessels increases during the inflammatory and proliferative phases, and then decreases as the wound enters the remodeling phase [79]. However, the mechanisms that lead to tortuous vessel resolution during the remodeling phase have not been addressed.

The wound healing response mimics the early stages of tumorigenesis in many ways, including the formation of tortuous vessels. The microenvironments of tumors and wounds share many similarities, including inflammation, hypoxia, and increased growth factor/cytokine signaling, and for this reason tumors have been described as "wounds that do not heal" [80]. However, a significant difference is that tortuous vessels in a wound environment resolve after the wound is healed, whereas cancer tortuous vessels maintain their tortuosity, possibly due to the constant secretion of growth factors by the tumor [81].

Current therapies to improve drug delivery to tumors are aimed at normalizing tortuous vessels surrounding tumors [82, 83]. Therefore, by understanding the process of tortuous vessel formation in an environment that is similar to cancer, but is able to repair itself, we can begin to unravel therapeutic targets towards tumor angiogenesis. Surprisingly, tortuous vessels have not been noted during development, even though growth factor signaling and hypoxic environments are present [84]. However, one component that is low during development, is the inflammatory response [43] which suggests that inflammation plays an important role in tortuous vessel formation.

1.4 BMP signaling in angiogenesis during development and disease

I have found that deletion of one of the BMP receptors, BMPR2, disrupts developmental angiogenesis. This section provides background on BMP signaling and what is known about BMPs and angiogenesis.

BMP signaling pathway

Bone morphogenetic proteins (BMP) are members of the transforming growth factor (TGF)-β superfamily, which includes TGF-β and activins. BMP ligands form hetero- or homodimers that bind to BMP receptors with varying affinity [85]. Ligands bind to heterotetrameric receptors made up of two type I and two type II BMP receptors. The type II receptor, BMPRII, is constitutively active and present as two variants, a short form and a long form that contains a long cytoplasmic tail [85]. Once in a complex, BMPRII phosphorylates type I receptors, initiating downstream canonical signaling through Smad transcription factors or non-canonically through MAPK/ERK [86]. Smad signaling is

initiated by phosphorylation of R-SMADs (SMAD 1/5/8) which then recruit SMAD4. This complex translocates to the nucleus and promotes transcription of downstream target genes, such as inhibitor of DNA binding 1 (Id1) [87]. Inhibitors regulate the BMP pathway at the extra- and intracellular level. Secreted antagonists, such as NOGGIN and CHORDIN, bind to BMP ligands and block their receptor binding sites [88]. Decoy receptors, such as BAMBI, compete with Type I receptors for complex formation with BMPRII and ligand binding [89]. SMAD6, an inhibitory Smad (I-Smad), can inhibit Smad signaling by binding to the R-Smad site on the Type I receptor, forming a non-functional complex with SMAD4, or interacting with transcriptional co-repressors in the nucleus [85]. At least twenty BMP ligands have been identified in mammals [10, 90]. Due to the large number of ligands and the dynamic interplay between ligand and receptor signaling, there are still many aspects of BMP signaling that continue to be revealed. Future work in illuminating BMP-signaling dynamics and disease relevance will be required to better understand this complex signaling pathway.

BMP signaling in angiogenesis

BMP ligands and receptors are expressed in endothelial cells during development and in adults [10, 91]. Recent studies have shown that some BMP ligands and receptors act as pro-angiogenic cues to induce sprouting angiogenesis [92-94]. For example, Bmp2b over-expression in zebrafish embryos causes ectopic vessel formation [95]. Interestingly, ectopic vessel formation is only induced from veins and occurs independently of VEGF signaling, indicating that BMP initiates sprouting in distinct vascular beds. Further studies in a human umbilical vein endothelial cell (HUVEC) based sprouting angiogenesis model show that BMP ligands promote lateral branching, implying that certain cells within a vessel are more

responsive to BMP and will sprout in a high BMP environment [96]. In another sprouting

HUVEC spheroid model, BMP4 ligand induces vessel sprouting via ERK signaling [90].

Additional studies show that the type I BMP receptor, ALK3, is recruited to the tips of

filopodia, thin actin based cell extensions that project from tip cells [97]. Dynamic filopodial

extensions that sense and respond to the microenvironment are associated with tip cells and

their forward migration. Pi et al. found that BMP6/ALK3 mediated signaling increased

filopodial extensions, driving endothelial cell migration. However, the BMP9/BMP10/ALK1

signaling axis has been shown to have an anti-angiogenic role. Using blocking antibodies

against BMP9, BMP10, or ALK1 injected into the postnatal retina, Ricard et al. found

disrupted vasculature, mainly an increase in vascular density [98]. Overall, these results

highlight the complexity of the BMP signaling pathway. Further studies are required to

understand the mechanisms of BMP-guided sprouting angiogenesis and to examine the

effects of BMP signaling in different vascular beds.

BMP signaling during disease and wound healing

In addition to angiogenesis, BMP signaling is also involved in maintaining

endothelial cell integrity in adult cells [91]. Haploinsufficiency for BMPR2 leads to

pulmonary arterial hypertension (PAH) in mice [99], a disease in which lung capillaries

become occluded, leading to increased blood pressure as the heart pumps harder to

compensate for the increased resistance. Additionally, loss of BMPR2 is associated with

increased inflammation. Studies performed by Kim et al. showed that deletion of BMPR2 in

HUVEC and human aortic endothelial cells (HAEC) lead to increased levels of inflammatory

markers such as vascular cell adhesion molecule 1 (VCAM-1) and intercellular adhesion

13

molecule 1 (ICAM-1) [100]. The authors used a heterozygous BMPR2 mutant mouse line to show that ICAM-1 and VCAM-1 were also upregulated in endothelial cells within the mouse thoracic aorta in this genetic background. Overall, these studies point to an important role for BMP signaling, and in particular BMPR2, in maintaining adult homeostasis.

During wound healing, BMP signaling activity becomes up-regulated in epithelial cells [101]. BMP2,4,6, and 7 are all expressed in wound tissue [102]. In particular, expression of BMP6 increases in keratinocytes and fibroblasts 2-3 days after an injury and regulates macrophage proliferation and dendrite cell maturation at the wound [103]. Studies in which downstream signaling components of the canonical BMP pathway were altered resulted in aberrant wound healing. Overexpression of Smad1 from keratinocytes resulted in increased apoptosis and decreased migration of wound epithelium as well as an inability to reorganize the cytoskeleton in epithelium, resulting in delayed wound healing [104]. Surprisingly, conditional deletion of Smad4 from the epidermis, also resulted in delayed wound healing [105]. However, in this case the delay is due to excessive inflammation and angiogenesis through upregulation of TGFβ1. Although BMP signaling has been studied during wound healing to some degree, the effects of BMPs on endothelial cells during wound healing remains relatively understudied.

1.5 Summary

Angiogenesis plays an important role during development, wound healing, and disease. Although, the signaling pathways contributing to angiogenesis are conserved, the outcomes of activating angiogenesis during development or disease can vary. Here, I show that endothelial specific deletion of *Bmpr2* in the postnatal retina leads to decreased

sprouting at the vascular front as well as branching in vascular plexus. These studies suggest that BMPR2 contributes to vascular patterning of the retina and is required for retinal sprouting angiogenesis.

A consequence of pro-angiogenic signaling during wound healing and disease is the formation of tortuous vessels. Tortuous vessels can be used as a therapeutic target to combat many diseases, ranging from cancer to diabetic ischemia. Thus, it is imperative to understand the mechanisms leading to tortuous vessel formation and resolution. Here, I provide a detailed investigation of tortuous microvessel (5-20 µm in diameter) formation and resolution at the cellular level during wound healing and analyze a new characteristic of tortuous microvessels, tortuous vessel sprouting.
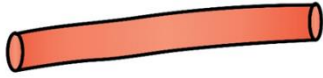
1.6 Figures

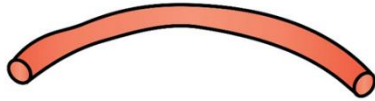**Figure 1.1 Morphology of normal and tortuous vessels.**

Normal vessels are linear or have a slight curve. Tortuous vessels have a sinusoidal S shape

or a kink.

Normal Vessels
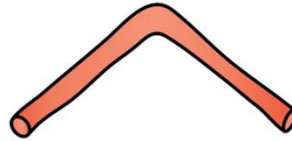
Tortuous Vessels

linear

slight
curve

curving
sinusoidal

kink

REFERENCES

1. Xu K, Cleaver O. Tubulogenesis during blood vessel formation. Seminars in cell & developmental biology. 2011;22(9):993-1004.

2. Stainier DY, Fouquet B, Chen JN, Warren KS, Weinstein BM, Meiler SE, et al. Mutations affecting the formation and function of the cardiovascular system in the zebrafish embryo. Development. 1996;123(1):285-292.

3. Rossant J. Mouse mutants and cardiac development: new molecular insights into cardiogenesis. Circ Res. 1996;78(3):349-353.

4. Risau W, Flamme I. Vasculogenesis. Annu Rev Cell Dev Biol. 1995;11:73-91.

5. Risau W. Mechanisms of angiogenesis. Nature. 1997;386(6626):671-674.

6. Cleaver O, Krieg PA. Chapter 8.2 - Vascular Development. Heart Development and Regeneration. Boston: Academic Press; 2010. p. 487-528.

7. Ferrara N, Gerber H-P, LeCouter J. The biology of VEGF and its receptors. Nat Med. 2003;9(6):669-676.

8. McColl BK, Stacker SA, Achen MG. Molecular regulation of the VEGF family -- inducers of angiogenesis and lymphangiogenesis. APMIS. 2004;112(7-8):463-480.

9. Ferrara N, Carver-Moore K, Chen H, Dowd M, Lu L, O'Shea KS, et al. Heterozygous embryonic lethality induced by targeted inactivation of the VEGF gene. Nature. 1996;380(6573):439-442.

10. Wiley DM, Jin SW. Bone Morphogenetic Protein functions as a context-dependent angiogenic cue in vertebrates. Semin Cell Dev Biol. 2011;22(9):1012-1018.

11. Herbert SP, Stainier DY. Molecular control of endothelial cell behaviour during blood vessel morphogenesis. Nat Rev Mol Cell Biol. 2011;12(9):551-564.

12. Chappell JC, Bautch VL. Vascular development: genetic mechanisms and links to vascular disease. Curr Top Dev Biol. 2010;90:43-72.

13. Chappell JC, Wiley DM, Bautch VL. Regulation of blood vessel sprouting. Semin Cell Dev Biol. 2011;22(9):1005-1011.

14. Lee CY, Bautch VL. Ups and downs of guided vessel sprouting: the role of polarity. Physiology (Bethesda). 2011;26(5):326-333.

15. Chappell JC, Wiley DM, Bautch VL. How Blood Vessel Networks Are Made and Measured. Cells, Tissues, Organs. 2011;195(1-2):94-107.

16.   Chappell JC, Taylor SM, Ferrara N, Bautch VL. Local Guidance of Emerging Vessel Sprouts Requires Soluble Flt-1 (VEGFR-1). Developmental cell. 2009;17(3):377-386.

17.   Kim J-D, Lee H-W, Jin S-W. Diversity Is in My Veins. Role of Bone Morphogenetic Protein Signaling During Venous Morphogenesis in Zebrafish Illustrates the Heterogeneity Within Endothelial Cells. 2014;34(9):1838-1845.

18.   Blanco R, Gerhardt H. VEGF and Notch in Tip and Stalk Cell Selection. Cold Spring Harbor Perspectives in Medicine. 2013;3(1):a006569.

19.   Adams RH, Alitalo K. Molecular regulation of angiogenesis and lymphangiogenesis. Nat Rev Mol Cell Biol. 2007;8(6):464-478.

20.   Chappell JC, Mouillesseaux KP, Bautch VL. Flt-1 (Vascular Endothelial Growth Factor Receptor-1) Is Essential for the Vascular Endothelial Growth Factor–Notch Feedback Loop During Angiogenesis. Arteriosclerosis, Thrombosis, and Vascular Biology. 2013;33(8):1952-1959.

21.   Kim J-D, Kang H, Larrivée B, Lee MY, Mettlen M, Schmid SL, et al. Context Dependent Pro-Angiogenic Function of Bone Morphogenetic Protein Signaling is Mediated by Disabled Homolog 2. Developmental cell. 2012;23(2):441-448.

22.   Boucher JM, Clark RP, Chong DC, Citrin KM, Wylie LA, Bautch VL. Dynamic alterations in decoy VEGF receptor-1 stability regulate angiogenesis. 2017;8:15699.

23.   Olsson AK, Dimberg A, Kreuger J, Claesson-Welsh L. VEGF receptor signalling - in control of vascular function. Nat Rev Mol Cell Biol. 2006;7(5):359-371.

24.   Fong G-H, Rossant J, Gertsenstein M, Breitman ML. Role of the Flt-1 receptor tyrosine kinase in regulating the assembly of vascular endothelium. Nature. 1995;376(6535):66-70.

25.   Kearney JB, Ambler CA, Monaco K-A, Johnson N, Rapoport RG, Bautch VL. Vascular endothelial growth factor receptor Flt-1 negatively regulates developmental blood vessel formation by modulating endothelial cell division. Blood. 2002;99(7):2397-2407.

26.   Shalaby F, Rossant J, Yamaguchi TP, Gertsenstein M, Wu XF, Breitman ML, et al. Failure of blood-island formation and vasculogenesis in Flk-1-deficient mice. Nature. 1995;376(6535):62-66.

27.   Dumont DJ, Jussila L, Taipale J, Lymboussaki A, Mustonen T, Pajusola K, et al. Cardiovascular Failure in Mouse Embryos Deficient in VEGF Receptor-3. Science. 1998;282(5390):946-949.

28.   Chung AS, Ferrara N. Developmental and pathological angiogenesis. Annu Rev Cell Dev Biol. 2011;27:563-584.

29. Keeley EC, Mehrad B, Strieter RM. Chemokines as Mediators of Neovascularization. Arteriosclerosis, Thrombosis, and Vascular Biology. 2008;28(11):1928-1936.

30. Singer AJ, Clark RAF. Cutaneous Wound Healing. New England Journal of Medicine. 1999;341(10):738-746.

31. Bielefeld KA, Amini-Nik S, Alman BA. Cutaneous wound healing: recruiting developmental pathways for regeneration. Cellular and Molecular Life Sciences. 2013;70(12):2059-2081.

32. Weis SM, Cheresh DA. Tumor angiogenesis: molecular pathways and therapeutic targets. Nature Medicine. 2011;17:1359+.

33. Reymond N, d'Agua BB, Ridley AJ. Crossing the endothelial barrier during metastasis. Nat Rev Cancer. 2013;13(12):858-870.

34. Tonnesen MG, Feng X, Clark RAF. Angiogenesis in Wound Healing. Journal of Investigative Dermatology Symposium Proceedings. 5(1):40-46.

35. Brem H, Tomic-Canic M. Cellular and molecular basis of wound healing in diabetes. J Clin Invest. 2007;117.

36. Tahergorabi Z, Khazaei M. Imbalance of angiogenesis in diabetic complications: the mechanisms. Int J Prev Med. 2012;3(12):827-838.

37. Wong VW, Crawford JD. Vasculogenic Cytokines in Wound Healing. BioMed Research International. 2013;2013:190486.

38. Greaves NS, Ashcroft KJ, Baguneid M, Bayat A. Current understanding of molecular and cellular mechanisms in fibroplasia and angiogenesis during acute wound healing. J Dermatol Sci. 2013;72(3):206-217.

39. Martin P, Nunan R. Cellular and molecular mechanisms of repair in acute and chronic wound healing. The British Journal of Dermatology. 2015;173(2):370-378.

40. Tonnesen MG, Feng X, Clark RA. Angiogenesis in wound healing. J Investig Dermatol Symp Proc. 2000;5.

41. Demidova-Rice TN, Durham JT, Herman IM. Wound Healing Angiogenesis: Innovations and Challenges in Acute and Chronic Wound Healing. Advances in Wound Care. 2012;1(1):17-22.

42. Koh TJ, DiPietro LA. Inflammation and wound healing: The role of the macrophage. Expert reviews in molecular medicine. 2011;13:e23-e23.

43. DiPietro LA. Angiogenesis and wound repair: when enough is enough. Journal of Leukocyte Biology. 2016;100(5):979-984.

44.   Barrientos S, Stojadinovic O, Golinko MS, Brem H, Tomic-Canic M. Growth factors and cytokines in wound healing. Wound Repair Regen. 2008;16.

45.   Bodnar RJ. Chemokine Regulation of Angiogenesis During Wound Healing. Advances in Wound Care. 2015;4(11):641-650.

46.   Barcelos LS, Duplaa C, Kränkel N, Graiani G, Invernici G, Katare R, et al. Human CD133(+) Progenitor Cells Promote the Healing of Diabetic Ischemic Ulcers by Paracrine Stimulation of Angiogenesis and Activation of Wnt Signaling. Circulation research. 2009;104(9):1095-1102.

47.   Galeano M, Torre V, Deodato B, Campo GM, Colonna M, Sturiale A, et al. Raxofelast, a hydrophilic vitamin E-like antioxidant, stimulates wound healing in genetically diabetic mice. Surgery. 2001;129(4):467-477.

48.   Moini M, Rasouli MR, Heidari P, Mahmoudi HR, Rasouli M. Role of early surgical revascularization in the management of refractory diabetic foot ulcers in patients without overt ischemic limbs. Foot Ankle Surg. 2010;16(1):50; author reply 51.

49.   Caravaggi C, Ferraresi R, Bassetti M, Sganzaroli AB, Galenda P, Fattori S, et al. Management of ischemic diabetic foot. J Cardiovasc Surg (Torino). 2013;54(6):737-754.

50.   Zhang J, Chen C, Hu B, Niu X, Liu X, Zhang G, et al. Exosomes Derived from Human Endothelial Progenitor Cells Accelerate Cutaneous Wound Healing by Promoting Angiogenesis Through Erk1/2 Signaling. Int J Biol Sci. 2016;12(12):1472-1487.

51.   Zhou J, Ni M, Liu X, Ren Z, Zheng Z. Curcumol Promotes Vascular Endothelial Growth Factor (VEGF)-Mediated Diabetic Wound Healing in Streptozotocin-Induced Hyperglycemic Rats. Med Sci Monit. 2017;23:555-562.

52.   Lord MS, Ellis AL, Farrugia BL, Whitelock JM, Grenett H, Li C, et al. Perlecan and vascular endothelial growth factor-encoding DNA-loaded chitosan scaffolds promote angiogenesis and wound healing. Journal of Controlled Release. 2017;250:48-61.

53.   Seo E, Lim JS, Jun J-B, Choi W, Hong I-S, Jun H-S. Exendin-4 in combination with adipose-derived stem cells promotes angiogenesis and improves diabetic wound healing. Journal of Translational Medicine. 2017;15(1):35.

54.   Han H-C. Twisted Blood Vessels: Symptoms, Etiology and Biomechanical Mechanisms. Journal of Vascular Research. 2012;49(3):185-197.

55.   McDonald DM, Baluk P. Imaging of angiogenesis in inflamed airways and tumors: newly formed blood vessels are not alike and may be wildly abnormal: Parker B. Francis lecture. Chest. 2005;128(6 Suppl):602S-608S.

56. Nagy JA, Chang SH, Dvorak AM, Dvorak HF. Why are tumour blood vessels abnormal and why is it important to know? British Journal of Cancer. 2009;100(6):865-869.

57. Schaper W, Scholz D. Factors Regulating Arteriogenesis. Arteriosclerosis, Thrombosis, and Vascular Biology. 2003;23(7):1143-1151.

58. Taarnhøj NCBB, Munch IC, Sander B, Kessel L, Hougaard JL, Kyvik K, et al. Straight versus tortuous retinal arteries in relation to blood pressure and genetics. British Journal of Ophthalmology. 2008;92(8):1055.

59. Jackson ZS, Dajnowiec D, Gotlieb AI, Langille BL. Partial Off-Loading of Longitudinal Tension Induces Arterial Tortuosity. Arteriosclerosis, Thrombosis, and Vascular Biology. 2005;25(5):957-962.

60. Dobrin PB, Schwarcz TH, Baker WH. Mechanisms of arterial and aneurysmal tortuosity. Surgery. 1988;104(3):568.

61. Nakamura T, Lozano PR, Ikeda Y, Iwanaga Y, Hinek A, Minamisawa S, et al. Fibulin-5/DANCE is essential for elastogenesis in vivo. Nature. 2002;415(6868):171-175.

62. Thurston G. Complementary actions of VEGF and Angiopoietin-1 on blood vessel growth and leakage. Journal of Anatomy. 2002;200(6):575-580.

63. Saaristo A, Veikkola T, Enholm B, HytÖNen M, Arola J, Pajusola K, et al. Adenoviral VEGF-C overexpression induces blood vessel enlargement, tortuosity, and leakiness but no sprouting angiogenesis in the skin or mucous membranes. The FASEB Journal. 2002;16(9):1041-1049.

64. Lee S, Jilani SM, Nikolova GV, Carpizo D, Iruela-Arispe ML. Processing of VEGF-A by matrix metalloproteinases regulates bioavailability and vascular patterning in tumors. The Journal of Cell Biology. 2005;169(4):681-691.

65. Han H-C. Blood vessel buckling within soft surrounding tissue generates tortuosity. Journal of Biomechanics. 42(16):2797-2801.

66. Park SO, Wankhede M, Lee YJ, Choi E-J, Fliess N, Choe S-W, et al. Real-time imaging of de novo arteriovenous malformation in a mouse model of hereditary hemorrhagic telangiectasia. The Journal of Clinical Investigation. 2009;119(11):3487-3496.

67. Krams R, Wentzel JJ, Oomen JA, Vinke R, Schuurbiers JC, de Feyter PJ, et al. Evaluation of endothelial shear stress and 3D geometry as factors determining the development of atherosclerosis and remodeling in human coronary arteries in vivo. Combining 3D reconstruction from angiography and IVUS (ANGUS) with computational fluid dynamics. Arterioscler Thromb Vasc Biol. 1997;17(10):2061-2065.

68. Qiao AK, Guo XL, Wu SG, Zeng YJ, Xu XH. Numerical study of nonlinear pulsatile flow in S-shaped curved arteries. Med Eng Phys. 2004;26(7):545-552.

69. Harry BL, Sanders JM, Feaver RE, Lansey M, Deem TL, Zarbock A, et al. Endothelial Cell PECAM-1 Promotes Atherosclerotic Lesions in Areas of Disturbed Flow in ApoE-Deficient Mice. Arteriosclerosis, thrombosis, and vascular biology. 2008;28(11):2003-2008.

70. Brooks AR, Lelkes PI, Rubanyi GM. Gene expression profiling of human aortic endothelial cells exposed to disturbed flow and steady laminar flow. Physiol Genomics. 2002;9(1):27-41.

71. Hayman DM, Zhang J, Liu Q, Xiao Y, Han H-C. Smooth Muscle Cell Contraction Increases the Critical Buckling Pressure of Arteries. Journal of biomechanics. 2013;46(4):841-844.

72. Fan L, Karino T. Effect of a disturbed flow on proliferation of the cells of a hybrid vascular graft. Biorheology. 2010;47(1):31-38.

73. Humbert M, Montani D, Perros F, Dorfmüller P, Adnot S, Eddahibi S. Endothelial cell dysfunction and cross talk between endothelium and smooth muscle cells in pulmonary arterial hypertension. Vascular Pharmacology. 2008;49(4–6):113-118.

74. Pietramaggiori G, Liu P, Scherer SS, Kaipainen A, Prsa MJ, Mayer H, et al. Tensile Forces Stimulate Vascular Remodeling and Epidermal Cell Proliferation in Living Skin. Annals of Surgery. 2007;246(5):896-902.

75. Hartnett ME, Martiniuk D, Byfield G, Geisen P, Zeng G, Bautch VL. Neutralizing VEGF Decreases Tortuosity and Alters Endothelial Cell Division Orientation in Arterioles and Veins in a Rat Model of ROP: Relevance to Plus Disease. Investigative ophthalmology & visual science. 2008;49(7):3107-3114.

76. Thurston G, Suri C, Smith K, McClain J, Sato TN, Yancopoulos GD, et al. Leakage-Resistant Blood Vessels in Mice Transgenically Overexpressing Angiopoietin-1. Science. 1999;286(5449):2511-2514.

77. Weinl C, Wasylyk C, Garcia Garrido M, Sothilingam V, Beck SC, Riehle H, et al. Elk3 deficiency causes transient impairment in post-natal retinal vascular development and formation of tortuous arteries in adult murine retinae. PLoS One. 2014;9(9):e107048.

78. Jung Y, Dziennis S, Zhi Z, Reif R, Zheng Y, Wang RK. Tracking dynamic microvascular changes during healing after complete biopsy punch on the mouse pinna using optical microangiography. PLoS One. 2013;8(2):e57976.

79. Rege A, Thakor NV, Rhie K, Pathak AP. In vivo laser speckle imaging reveals microvascular remodeling and hemodynamic changes during wound healing angiogenesis. Angiogenesis. 2012;15(1):87-98.

80.   Dvorak HF. Tumors: wounds that do not heal. Similarities between tumor stroma generation and wound healing. N Engl J Med. 1986;315(26):1650-1659.

81.   Witsch E, Sela M, Yarden Y. Roles for Growth Factors in Cancer Progression. Physiology (Bethesda, Md). 2010;25(2):85-101.

82.   Goel S, Wong AH-K, Jain RK. Vascular Normalization as a Therapeutic Strategy for Malignant and Nonmalignant Disease. Cold Spring Harbor Perspectives in Medicine. 2012;2(3):a006486.

83.   Huang Y, Yuan J, Righi E, Kamoun WS, Ancukiewicz M, Nezivar J, et al. Vascular normalizing doses of antiangiogenic treatment reprogram the immunosuppressive tumor microenvironment and enhance immunotherapy. Proceedings of the National Academy of Sciences of the United States of America. 2012;109(43):17561-17566.

84.   Dunwoodie SL. The Role of Hypoxia in Development of the Mammalian Embryo. Developmental Cell. 17(6):755-773.

85.   Sieber C, Kopf J, Hiepen C, Knaus P. Recent advances in BMP receptor signaling. Cytokine & Growth Factor Reviews. 2009;20(5–6):343-355.

86.   Nohe A, Keating E, Knaus P, Petersen NO. Signal transduction of bone morphogenetic protein receptors. Cellular Signalling. 2004;16(3):291-299.

87.   Korchynskyi O, ten Dijke P. Identification and Functional Characterization of Distinct Critically Important Bone Morphogenetic Protein-specific Response Elements in the Id1 Promoter. Journal of Biological Chemistry. 2002;277(7):4883-4891.

88.   Liu A, Niswander LA. Bone morphogenetic protein signalling and vertebrate nervous system development. Nat Rev Neurosci. 2005;6(12):945-954.

89.   Cai J, Pardali E, Sanchez-Duffhues G, ten Dijke P. BMP signaling in vascular diseases. FEBS Lett. 2012;586(14):1993-2002.

90.   Zhou Q, Heinke J, Vargas A, Winnik S, Krauss T, Bode C, et al. ERK signaling is a central regulator for BMP-4 dependent capillary sprouting. Cardiovascular Research. 2007;76(3):390-399.

91.   Wang RN, Green J, Wang Z, Deng Y, Qiao M, Peabody M, et al. Bone Morphogenetic Protein (BMP) signaling in development and human diseases. Genes & diseases. 2014;1(1):87-105.

92.   Beets K, Huylebroeck D, Moya IM, Umans L, Zwijsen A. Robustness in angiogenesis: Notch and BMP shaping waves. Trends in Genetics. 29(3):140-149.

93.   Dyer LA, Pi X, Patterson C. The role of BMPs in endothelial cell function and dysfunction. Trends in endocrinology and metabolism: TEM. 2014;25(9):472-480.

94. David L, Feige JJ, Bailly S. Emerging role of bone morphogenetic proteins in angiogenesis. Cytokine Growth Factor Rev. 2009;20(3):203-212.

95. Wiley DM, Kim J-D, Hao J, Hong CC, Bautch VL, Jin S-W. Distinct Signaling Pathways Regulate Sprouting Angiogenesis from the Dorsal Aorta and Axial Vein. Nature cell biology. 2011;13(6):686-692.

96. Mouillesseaux KP, Wiley DS, Saunders LM, Wylie LA, Kushner EJ, Chong DC, et al. Notch regulates BMP responsiveness and lateral branching in vessel networks via SMAD6. Nature Communications. 2016;7:13247.

97. Pi X, Ren R, Kelley R, Zhang C, Moser M, Bohil AB, et al. Sequential roles for myosin-X in BMP6-dependent filopodial extension, migration, and activation of BMP receptors. The Journal of Cell Biology. 2007;179(7):1569-1582.

98. Ricard N, Ciais D, Levet S, Subileau M, Mallet C, Zimmers TA, et al. BMP9 and BMP10 are critical for postnatal retinal vascular remodeling. Blood. 2012;119(25):6162-6171.

99. Morrell NW. Pulmonary Hypertension Due to BMPR2 Mutation. Proceedings of the American Thoracic Society. 2006;3(8):680-686.

100. Kim CW, Song H, Kumar S, Nam D, Sang Kwon H, Hwa Chang K, et al. Anti-Inflammatory and Antiatherogenic Role of BMP Receptor II in Endothelial Cells. Arteriosclerosis, Thrombosis, and Vascular Biology. 2013.

101. Sountoulidis A, Stavropoulos A, Giaglis S, Apostolou E, Monteiro R, Chuva de Sousa Lopes SM, et al. Activation of the canonical bone morphogenetic protein (BMP) pathway during lung morphogenesis and adult lung tissue repair. PLoS One. 2012;7(8):e41460.

102. Wankell M, Munz B, Hubner G, Hans W, Wolf E, Goppelt A, et al. Impaired wound healing in transgenic mice overexpressing the activin antagonist follistatin in the epidermis. EMBO J. 2001;20(19):5361-5372.

103. Kaiser S, Schirmacher P, Philipp A, Protschka M, Moll I, Nicol K, et al. Induction of Bone Morphogenetic Protein-6 in Skin Wounds. Delayed Reepitheliazation and Scar Formation in BMP-6 Overexpressing Transgenic Mice. Journal of Investigative Dermatology. 111(6):1145-1152.

104. Lewis CJ, Mardaryev AN, Poterlowicz K, Sharova TY, Aziz A, Sharpe DT, et al. Bone morphogenetic protein signalling suppresses wound-induced skin repair by inhibiting keratinocyte proliferation and migration. The Journal of investigative dermatology. 2014;134(3):827-837.

105. Owens P, Engelking E, Han G, Haeger SM, Wang X-J. Epidermal Smad4 Deletion Results in Aberrant Wound Healing. The American Journal of Pathology. 2010;176(1):122-133.

Chapter 2: Alk2/ACVR1 and Alk3/BMPR1A Provide Essential Function for Bone Morphogenetic Protein Induced Retinal Angiogenesis[1]

2.1 Summary

Increasing evidence suggests that Bone Morphogenetic Protein (BMP) signaling regulates angiogenesis. Here, we aimed to define the function of BMP receptors in regulating early post-natal angiogenesis by analysis of inducible, endothelial specific deletion of the BMP receptor components *Bmpr2*, *Alk1*, *Alk2* and *Alk3* in mouse retinal vessels. Expression analysis of several BMP ligands showed that pro-angiogenic BMP ligands are highly expressed in postnatal retinas. Consistently, BMP receptors are also strongly expressed in retina with a distinct pattern. To assess the function of BMP signaling in retinal angiogenesis, we first generated mice carrying an endothelial-specific inducible deletion of BMP Type 2 receptor (*Bmpr2*). Postnatal deletion of *Bmpr2* in endothelial cells substantially decreased the number of angiogenic sprouts at the vascular front and branchpoints behind the front, leading to attenuated radial expansion. To identify critical BMPR1s associated with BMPR2 in retinal angiogenesis, we generated endothelial-specific inducible deletion of three BMPR1s abundantly expressed in endothelial cells and analyzed the respective phenotypes. Among these, endothelial specific deletion of either *Alk2*/*acvr1* or *Alk3*/*Bmpr1a* caused a delay in

---

radial expansion, reminiscent of vascular defects associated with postnatal endothelial specific deletion of BMPR2, suggesting that ALK2/ACVR1 and ALK3/BMPR1A are likely to be the critical BMPR1s necessary for pro-angiogenic BMP signaling in retinal vessels. Our data identify BMP signaling mediated by coordination of ALK2/ACVR1, ALK3/BMPR1A, and BMPR2 as an essential pro-angiogenic cue for retinal vessels.

2.2 Introduction

Bone Morphogenetic Protein (BMP) signaling has been implicated as a key regulator for angiogenesis [1]. Depending on the nature of the ligands, BMP signaling can either promote or inhibit angiogenesis [2]; Pro-angiogenic BMP2/4 augments vessel sprouting in a matrigel plug assay [3], and stimulation with BMP2 promotes angiogenic responses such as filopodia extension and migration in human umbilical vein endothelial cells (HUVEC) by inducing the expression of target genes, such as *MYOX* [4]. In addition, its zebrafish orthologue, Bmp2b, functions as the predominant angiogenic cue for veins [5, 6]. Similar pro-angiogenic effects have been demonstrated for BMP6 [4, 7]. In contrast, BMP9 and BMP10 induce quiescence of endothelial cells, and therefore function as anti-angiogenic cues [8-10]. Consistent with the idea that BMP9 and BMP10 modulate the homeostasis of mature vessels, it has been shown that BMP9 can promote differentiation of endothelial progenitors during ischemic neovascularization [11].

On the cell membrane of the signal receiving cells, BMP ligands interact with tetra-heteromeric receptor complexes composed of two BMP Type 1 Receptors (BMPR1s) and two BMP Type 2 Receptors (BMPR2s). The signaling specificity of each BMP ligand is

27

determined by the interaction between BMP ligand and its cognate BMPR1, since BMPR2 can only serve as a low affinity receptor [12, 13]. Therefore, BMPR1s are essential for the outcomes of BMP signaling. In the mammalian genome, four BMPR1s, *Alk1/Acvrl1*, *Alk2/Acvr1*, *Alk3/Bmpr1a*, and *Alk6/Bmpr1b*, have been annotated [14, 15]. Previous work showed that endothelial-specific deletion of *Alk1* generates exuberant angiogenesis, indicating that ALK1 is likely to mediate anti-angiogenic BMP9/10 signaling in endothelial cells [9, 16, 17]. Considering that ALK2, ALK3, and ALK6 bind to BMP2, BMP4, and BMP6 in other circumstances [18], these receptors are likely to mediate pro-angiogenic BMP signaling. However, since global deletion of these receptors leads to early embryonic lethality [19-22], surprisingly little is known about the individual function of these BMPR1s in endothelial cells. In addition, previous attempts to elucidate the role of each BMPR1 in endothelial cells failed to provide comprehensive analyses due to the lack of suitable endothelial-specific Cre driver lines [23, 24]. Most importantly, manipulations of BMPR1 in endothelial cells were not performed in the same way in the same vascular bed in previous studies, making it difficult to determine the role of each BMPR1s in endothelial cells [23, 24].

In this study, we investigated the function of each BMPRI in angiogenesis using postnatal mouse retinal vessels to better understand the molecular and cellular underpinning of pro-angiogenic BMP signaling. To assess the contribution of BMPs in retinal angiogenesis, we showed BMP signaling reporter activity in the early postnatal retina, and found that BMP6 and BMP7 are the most abundant BMP ligands in that organ. We found that several BMPR1s were expressed in distinct regions of the retinal vasculature. Conditional deletion of *Bmpr2* and three highly expressed BMPRIs, *Alk1/Acvrl1*, *Alk2/Acvr1*,

and *Alk3/Bmpr1a*, in endothelial cells of postnatal mice showed that mice deficient for *Alk2/Acvr1* or *Alk3/Bmpr1a* partially phenocopied the vascular defects of mice with an endothelial specific deletion of *Bmpr2*. Taken together, our data indicate that the pro-angiogenic BMP signaling mediated by ALK2 and ALK3 receptors, likely in conjunction with BMPR2, is essential for proper retinal angiogenesis.

2.3 Materials and Methods

Genetic experiments and pharmacological inhibition

All animal procedures were performed in accordance with Yale University and University of North Carolina Institutional Animal Care and User Committee guidelines. The following mouse strains were used: *Alk1$^{fl/fl}$* [25], *Alk2$^{fl/fl}$* [26], *Alk3$^{fl/fl}$* [27], *Bmpr2$^{fl/fl}$* [28], and *Cdh5(Pac)Cre^{ERT2}* [29], and BRE-gfp [30] mice. For endothelial-cell-specific loss-of-function of BMPRs, mice carrying homozygous floxed alleles of BMPR were interbred with Cdh5(Pac)CreERT2 mice. All of the mouse strains were back-crossed into the C57Bl/6J background. Genetic modifications were induced by intraperitoneal injections with 30 or 100μg tamoxifen (Sigma) at P1 and P2.

Isolation of mouse endothelial cell and manipulation of mouse retina

Mouse lung endothelial cells (MLECs) for qRT-PCR analyses were isolated as described previously [31, 32]. In total, six P6 pups were euthanized by decapitation. The lungs were removed and placed in a 1.5mL eppendorf tube. Lungs were finely minced with sharp scissors, then the tissue was digested with 2mg/mL collagenase type I in PBS at 37°C

29

for 45 min. The digest was passed through a 75μm cell strainer to remove undigested tissue fragments. Cells were pelleted at 400 g for 5 minutes, resuspended in 2% FBS containing PBS with magnetic beads-coated rat anti-mouse CD31 (PECAM-1) antibody (Ab) (BD PharMingen). After incubation on room temperature for 12 min, the cells were placed on the magnet for 5 min and unbound cells were removed. The bound cells were resuspended in medium and plated onto a 0.1% gelatin-coated dish. Mouse retina dissection and manipulation was performed as previously reported [33].

Immunofluorescence (IF)

The following antibodies were used: anti-ALK1 (1:100, R&D Systems), anti-ALK2 (1:100, Proteintech), anti-ALK3 (1:100, Thermo), anti-BMPR2 (1:100, BD), anti-PECAM-1 (1:200, BD) and isolectin-B4 (1:100, BD). Alexa Fluor 488, 555 and 647 donkey secondary antibodies were from Invitrogen. Retina immunostaining was carried out with littermates processed simultaneously under the same conditions. To analyze and quantify the retina vascular phenotype, the eyes were fixed in 4% PFA for 2 hours at 4°C and dissected as previously reported (REF). After washing the retinas were permeabilized using PBS-T (0.1% Triton X-100 containing PBS) and incubated overnight at 4°C in PBS-T containing biotinylated isolectin B4 (IB4) and the primary antibodies. Then the retinas were incubated with fluorophore-conjugated antibodies and with Alexa Fluor 488/555/647 (Invitrogen), and mounted with Fluorescence Mounting Medium (Dako). Confocal microscopy was performed with Leica SP5 confocal microscopes. ImageJ (NIH) was used for the data analysis. The figures were assembled using Adobe Photoshop. The only adjustments used in the preparation of the figures were for brightness and contrast. RT-PCR For gene expression

analysis, the total RNA was isolated with RNeasy Mini kits (QIAGEN) and 1 μg total RNA

was reverse transcribed using High-Capacity cDNA Reverse Transcription Kit (Thermofisher

scientific) following the manufacturer instructions. The cDNAs were amplified using the FG

Power SYBR Green PCR Master Mix (Applied Biosystems) in an Eppendorf Mastercycler

gradient. The relative expression differences represent the means of the results obtained from

at least three-independent experiments.

Statistical analysis

Data are expressed as mean ± SEM. Comparisons between groups were made using a

two-tailed Student t test. Prior to the student t test, we have used the Levene's test to examine

whether the assumptions and conditions for t test were violated, and therefore, could not be

used to determine the differences between groups. We found that knockout mice and

phenotypic wild-type siblings are statistically indistinguishable groups for a number of

unrelated parameters. In all parameters we used, the F values were significantly smaller than

the Table F value at α=0.001. Our statistical analyses demonstrated that knockout mice and

their phenotypic wild-type siblings have similar population variances, and therefore, the

assumptions and conditions for t test was not violated. This result supports our approach to

employ t test to perform statistical analyses.

2.4 Results

Diverse BMP ligands and receptors are expressed during retinal angiogenesis

To determine the role of pro-angiogenic BMP signaling, we first examined the

expression of GFP in retinal vessels of BRE-GFP mice, where the expression of GFP is

regulated by BMP Responsive Elements (BRE) isolated from the *Id1* promoter [34]. As previously reported [30], BRE-GFP expression was broadly detected in P5 retinal vessels (**Figure 2.1A**). Within the vascular front, BRE-GFP was highly expressed in both tip and stalk cells (**Figure 2.1B**). While the expression of BRE-GFP in stalk cells can be attributed to the ALK1-mediated anti-angiogenic BMP signaling activity [9, 30], it is not clear how BRE-GFP expression in tip cells is induced.

To identify which BMP ligands and receptors induce BRE-GFP expression in the retinal vessels, we performed *in situ* hybridization analyses on mouse retinas and quantitative RT-PCR using cells isolated from postnatal retinas at different developmental stages (**Figure 2.1C** and **Supplementary Figure 2.1**). A number of pro-angiogenic BMP ligands were highly expressed during the stages coincident with extensive retinal angiogenesis (**Figure 2.1C** and **Supplementary Figure 2.2**). In particular, the expression of BMP6 and BMP7, was increased over two folds. In contrast, expression of BMP9 and 10, which are ligands for ALK1 and are produced by liver and heart respectively, were not detected in the retina (**Supplementary Figure 2.1**). However, given that they are delivered by circulation, it is likely that the mature BMP9 and BMP10 protein are present in the retina. In endothelial cells, only three BMPR1s, ALK1, ALK2, and ALK3, but not ALK6, were highly expressed. Therefore, ALK6 was excluded from further analyses (**Supplementary Figure 2.3**).

Next, we analyzed the expression of BMPR2 and the three BMPR1s that are abundant in endothelial cells, ALK1/ACVRL, ALK2/ACVR1A, and ALK3/BMPR1A by immunostaining in retinas (**Figure 2.1D-G** and data not shown). BMPR2 staining is vascular and appears in all vessels, with heightened expression at the vascular front (**Figures 2.1D and H**). Interestingly, each BMPR1 has distinct expression pattern; ALK1 and ALK3

proteins are found in both plexus and vascular front, with ALK1 being enriched in the arteries of the plexus region. ALK2 staining is highly enriched in veins in the plexus region and not associated with the vascular front or arteries (**Figures 2.1E-G** and **I-K**). These findings show that pro-angiogenic BMP ligands and receptors are highly expressed in blood vessels during retinal development, and the receptors have distinct expression patterns. Therefore, it is likely that BRE-GFP reporter activity in tip cells at the vascular front results from the activity of proangiogenic BMP ligands.

BMPR2 activity promotes retinal angiogenesis

To examine the requirement for pro-angiogenic BMP signaling during retinal angiogenesis, we generated mice carrying an inducible, endothelial-specific *Bmpr2* deletion by crossing *Bmpr2$^{fl/fl}$* and *Cdh5(Pac)Cre^{ERT2}* mice27. Given that BMPR2 is the predominant binding partner for BMPR1s mediating pro-angiogenic BMP activity, we postulated that deletion of *Bmpr2* is likely to attenuate signaling outcomes downstream of most pro-angiogenic BMP ligand engagement during retinal angiogenesis. Consistent with our hypothesis, endothelial cell deletion of *Bmpr2* significantly decreased the radial expansion of the retinal vessels (**Figures 2.2A** and **C**), indicating that BMP signaling is essential for retinal angiogenesis. *Bmpr2$^{fl/fl}$;Cdh5(Pac)Cre^{ERT2}* mice also displayed a significant reduction in vascular density (% vascularized area) compared to wild-type littermates (**Figures 2.2B** and **C**). This data shows that pro-angiogenic BMP signaling mediated by BMPR2 is a critical positive regulator of retinal angiogenesis.

Endothelial specific deletion of Alk2/ACVR1A or Alk3/BMPR1A but not Alk1/ACVRL recapitulates vascular defects of endothelial specific deletion of Bmpr2

Next, we investigated critical BMPR1 interactions mediating pro-angiogenic BMP signaling during retinal angiogenesis. Endothelial deletion of *Alk1*, *Alk2*, or *Alk3* during postnatal retinal angiogenesis was induced by crossing homozygous mice carrying a floxed allele of each *BMPR1* and *Cdh5(Pac)Cre^{ERT2}* mice (**Supplementary Figure 2.4**). As previously reported [9, 29], tamoxifen-mediated deletion7 of *Alk1* in endothelial cells at P1 did not exhibit severe defects in radial extension, but caused exuberant angiogenesis in developing retinas compared to phenotypic wild-type littermates and therefore substantially increased vascular density (% vascularized area) (**Figure 2.3A, D**). In *Alk1$^{fl/fl}$;Cdh5(Pac)Cre^{ERT2}* mice, the vascular phenotype was more pronounced in the vascular front than in the plexus region (**Figure 2.3A**). Considering the distinct phenotypes between *Bmpr2$^{fl/fl}$;Cdh5(Pac)Cre^{ERT2}* and *Alk1$^{fl/fl}$;Cdh5(Pac)Cre^{ERT2}* mice, it is unlikely that ALK1 is involved in pro-angiogenic BMP signaling mediated by BMPR2.

In contrast, tamoxifen-mediated deletion of *Alk2* or *Alk3* in endothelial cells at P1 led to a substantial reduction in the radial expansion of retinal vessels (**Figures 2.3B**-**C** and **Supplementary Figure 2.4**), reminiscent of the defects in *Bmpr2$^{fl/fl}$;Cdh5(Pac)Cre^{ERT2}* mice (**Figure 2A**). In addition, vascular density was substantially reduced in tamoxifen-injected *Alk2$^{fl/fl}$;Cdh5(Pac)Cre^{ERT2}* or *Alk3$^{fl/fl}$;Cdh5(Pac)Cre^{ERT2}* retinas compared to wild-type littermates (**Figure 2.3D**). These findings show that both ALK2 and ALK3 are important for proper retinal vessel morphogenesis, likely in conjunction with BMPR2.

Endothelial specific deletion of Alk3/BMPR1A and Bmpr2 but not Alk2/ACVR1A affect angiogenic sprouts at the vascular front

Considering that both *Alk2* and *Alk3* deletion in endothelial cells significantly delayed radial expansion but only *Alk3* is expressed at the vascular front, we hypothesized that ALK2 and ALK3 receptors would differentially affect angiogenic sprouts. To examine this notion, we first examined the phenotype of endothelial deletion of *Bmpr2* and found that lack of *Bmpr2* significantly decreased the number of angiogenic sprouts (**Figure 2.4A**). Endothelial deletion of *Alk3*/*BMPR1A* similarly decreased the number of angiogenic sprouts present at the vascular front compared to phenotypic wild-type littermates (**Figures 2.4B** to **C**), while deletion of *Alk2* did not significantly alter the number of angiogenic sprouts at the vascular front. Considering that the vascular coverage (% vascularized area) was significantly decreased in retinas of mice with deletion of either receptor (**Figure 2.3B-D**), it is likely that different BMPR1 receptors mediate pro-angiogenic BMP signaling at the vascular front and behind the front.

2.5 Discussion

Our results identify BMPR2/ALK2 and BMPR2/ALK3 as key receptors that mediate pro-angiogenic BMP signaling in the early post-natal retina, and reveal regional differences among BMPR1s by analysis of parallel genetic experiments in a defined vascular bed. Deletion of the common BMPR2 receptor reduced vascular sprouting and density. Deletion of ALK3, which is ubiquitously expressed in retinal endothelial cells, also dramatically reduced vascular sprouting and density, while loss of ALK2, which is enriched behind the vascular front, did not significantly affect sprouting but reduced overall vessel density.

Therefore, we propose that spatially regulated BMPR1 expression fine-tunes endothelial cell responses to pro-angiogenic BMP ligands in development. Since expression of BMP ligands selective for ALK2 and ALK3 is elevated during retinal angiogenesis, it is tempting to speculate that BMP6/7-ALK2/3-BMPR2 signaling axis may provide essential input for the developing retina.

Since the phenotype of endothelial-specific deletion of *Bmpr2* is quite distinct from the vascular phenotype caused by endothelial-specific deletion of *Alk1*, it is likely that BMPR2-mediated proangiogenic signaling is dominant over interactions with ALK1 in the early postnatal retina. In contrast, ALK2 and ALK3 appear to be essential for BMPR2-mediated pro-angiogenic signaling. These receptors function similarly but non-redundantly behind the vascular front in mediating branching, as deletion of either Type 1 receptor partially phenocopies the phenotype of *Bmpr2* deletion and results in reduced branching. This finding suggests that both ALK2/BMPR2 and ALK3/BMPR2 complexes contribute to branching morphogenesis, which is consistent with our previous finding that proangiogenic BMP signaling leads to increased branching *in vitro* and *in vivo* [5, 6]. Angiogenic sprouting at the vascular front is likely to selectively utilize ALK3/BMPR2 complexes, since genetic deletion of *Alk2* did not significantly affect angiogenic sprouting. This is consistent with the expression patterns of the receptors in the early postnatal retina, as ALK3 but not ALK2 reactivity was found at the vascular front. ALK2 reactivity is enriched in veins, while ALK3 expression is not enriched in larger vessels, suggesting potential differences in ALK2 and ALK3 mediated pro-angiogenic BMP signaling.

ALK1, which does not appear to be essential for BMPR2-mediated pro-angiogenic BMP signaling, may provide an additional regulation for vessel remodeling and homeostasis at later stages.

Previously, it has been shown that BMPR1s can promiscuously form heterodimeric complex [16, 35-37]. For instance, it has been shown that ALK1 and ALK2 can form heterodimers under certain circumstances [36, 37]. Similarly, ALK2 and ALK3 are proposed to form heterodimers to mediate BMP2 signaling [35]. Therefore, it is possible that they may influence the signaling property of each other. While we cannot rule of this possibility due to the lack of appropriate reagents, given the distinct expression pattern of BMPR1s, we believe that the vascular phenotype caused by endothelial specific deletion of single BMPR1 is likely to represent the unique signaling property of each receptor.

Our analyses indicate that ALK3/BMPR2 mediated BMP signaling regulates angiogenic sprouting at the vascular front, while both ALK3/BMPR2 and ALK2/BMPR2 regulate branching behind the vascular front. This is consistent with our finding that BMP signaling, as read out by BRE-EGFP, is active throughout the retinal vasculature, and suggests that pro-angiogenic BMP signaling regulates both sprouting and branching. These results are consistent with a previous report describing ubiquitous expression of BRE-EGFP in retinal vessels [30].

Our work presents compelling evidence that pro-angiogenic BMP signaling is important for angiogenesis. Here we show that expression of Type 1 receptors, specifically ALK2 and ALK3, may explain the different effects of BMP signaling on developing vessels, and they each likely complex with BMPR2 to mediate pro-angiogenic effects in blood vessels in a non-redundant way. While the molecular underpinning of the phenotypic

differences between *Alk2fl/fl*;*Cdh5(Pac)CreERT2* and *Alk3fl/fl*;*Cdh5(Pac)CreERT2* mice

needs further analyses, careful phenotypic comparisons between these mice will help

elucidate how angiogenesis is regulated in development and disease, and may provide useful

information in developing therapeutic strategies.

2.6 Figures

Figure 2.1. Diverse BMP ligands and receptors are expressed during retinal development

(A-B) Representative overview of retinal vessels at (A) the retinal center and (B) vascular front shown in higher magnification in postnatal day P5 BRE-gfp transgenic mice. Endothelial cells are shown in red. BRE-GFP is highly expressed in both tip cells and stalk cells. (C) qRT-PCR for Bmp ligands and Vegfa in P0, P2, P4, and P6 retina. Bmp6 and Bmp7 are the most abundant BMP ligands between P0 and P6 (n=5). (D-G) Immunohitochemistry of P5 retina showing BMPR2 (D), ALK1/ACVRL (E), ALK2/ACVR1 (F), and ALK3/BMPR1A (G). While BMPR2, ALK1 and ALK3 are expressed ubiquitously, ALK2 expression is enriched in the veins within the plexus region; scale bar, 300μm. (H-K) Areas within the white rectangles in panels D to G are shown in higher magnification.
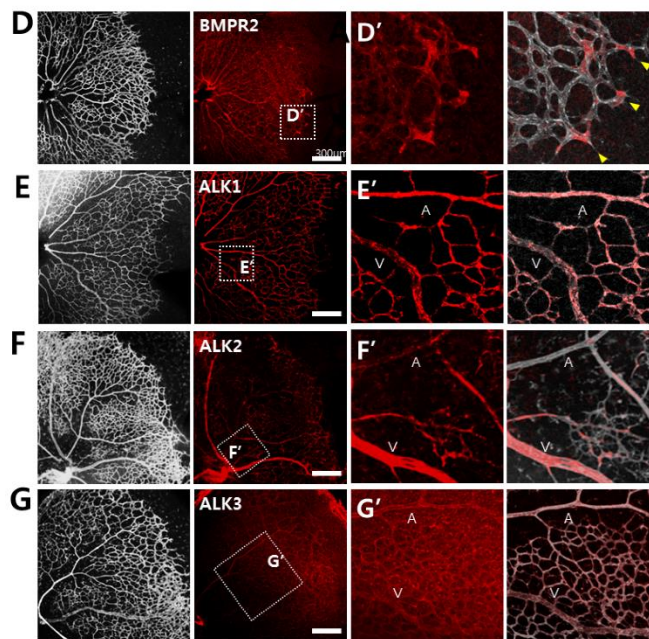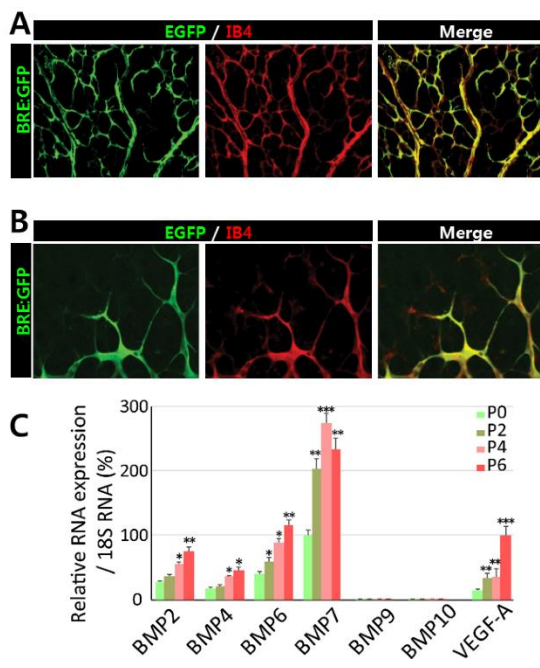
Figure 2.2. BMPR2 is essential for retinal angiogenesis

(A) Representative overview of P5 retinal vessels taken from inducible endothelial specific knock out of $Bmpr2^{fl/fl};Cdh5(Pac)Cre^{ERT2}$ (right) and their phenotypic wild-type littermates (left); scale bar, 500µm. Mean radial expansion of the retinal vessels in P5 $Bmpr2^{fl/fl}$ retinas was decreased to 78.9±9.8% of wildtype littermates. (B) Representative overview of plexus region of P5 retina in $Bmpr2^{fl/fl};Cdh5(Pac)Cre^{ERT2}$ (right) and their phenotypic wild-type littermates (left). Mean vascular density in the plexus region in Bmpr2fl/fl retinas was reduced to 65.7±8.3% of wildtype littermates; scale bar, 500µm. Endothelial cells are visualized by anti- Isolectin B4 (IB4) staining. (C) Quantification of radial expansion and vascular density (% vascularized area) in $Bmpr2^{fl/+};Cdh5(Pac)Cre^{ERT2}$ (gray) and $Bmpr2^{fl/fl};Cdh5(Pac)Cre^{ERT2}$ mice injected with 100µg tamoxifen at P1, retinas were assayed P5 (n=5). P<0.05. Statistical significance was assessed using a Student's unpaired t-test.
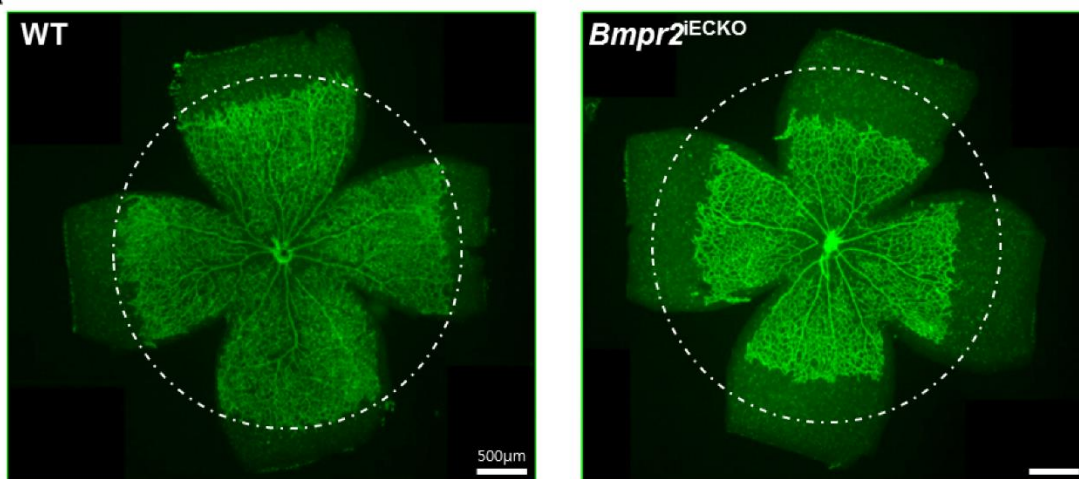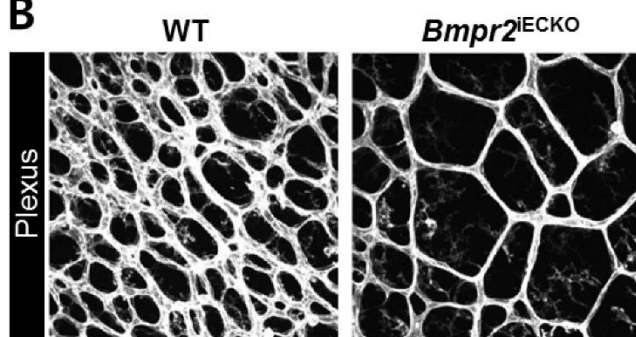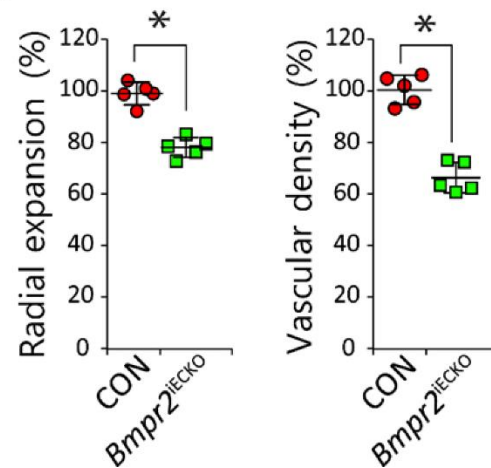
A

WT   *Bmpr2*^iECKO

500μm

B

Plexus   WT   *Bmpr2*^iECKO

C

Radial expansion (%)

CON   *Bmpr2*^iECKO

Vascular density (%)

CON   *Bmpr2*^iECKO

Figure 2.3. ALK2 and ALK3 promotes retinal angiogenesis

(A-C) Representative overview of retinal vessels taken from inducible endothelial specific knock out of *Alk1$^{fl/fl}$;Cdh5(Pac)Cre^{ERT2}* (A), *Alk2$^{fl/fl}$;Cdh5(Pac)Cre^{ERT2}* (B), or *Al31$^{fl/fl}$;Cdh5(Pac)Cre^{ERT2}* (C) and their phenotypic wild-type littermates. Mice were injected with 50μg tamoxifen at P1, retinas were assayed P5; scale bar, 500μm. Both radial expansion and vascular density in the plexus region were significantly increased in P5 *Alk1$^{fl/fl}$;Cdh5(Pac)Cre^{ERT2}* retinas (101±6.7% for radial expansion and 155±6.2% for vascular density compared to wildtype littermates). By contrast, deletion of either *Alk2* or *Alk3* significantly decreased both radial expansion (63.2±17.1% for Alk2fl/f;Cdh5(Pac)CreERT2 retinas and 56.4±14.2% for *Alk3$^{fl/fl}$;Cdh5(Pac)Cre^{ERT2}* retinas compared to wildtype littermates) and vascular density in the plexus region (42.3±15.9% for *Alk2$^{fl/fl}$;Cdh5(Pac)Cre^{ERT2}* retinas, and 61.9±12.8% for *Alk3$^{fl/fl}$;Cdh5(Pac)Cre^{ERT2}* retinas compared to wildtype littermates). Areas within the white rectangle in middle column are shown in higher magnification (right column). While radial expansion was similarly affected by deletion of either *Alk2* or *Alk3*, vascular density in the plexus region is more severely affected by the deletion of *Alk2* than *Alk3*. Endothelial cells are visualized by anti- Isolectin B4 (IB4) staining. (D) Quantification of radial expansion and vascular density (% vascularized area) in inducible endothelial specific knockout of each *BMPR1* (pink) and their littermates (gray) (n=5). P<0.05. Statistical significance was assessed using a Student's unpaired t-test.
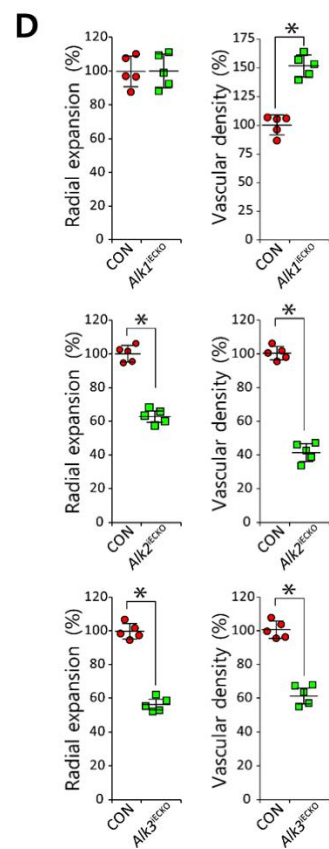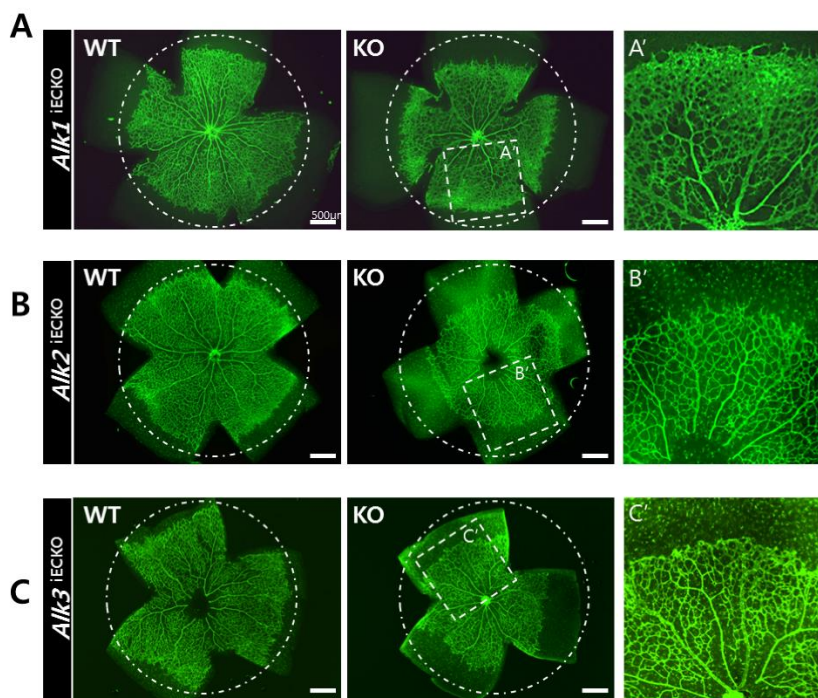
Figure 2.4. ALK3/BMPR2 signaling is required for the formation of angiogenic sprouts in the vascular front

(A) Representative image of vascular front in postnatal day P5 *Bmpr2$^{fl/fl}$;Cdh5(Pac)Cre^{ERT2}* (A), *Alk2$^{fl/fl}$; Cdh5(Pac)Cre^{ERT2}* (B), or *Alk3$^{fl/fl}$; Cdh5(Pac)Cre^{ERT2}* Endothelial cells are visualized by anti-Isolectin B4 (IB4) staining. (C) and their phenotypic wild-type littermates. Green arrows point the angiogenic sprouts in the vascular front (n=5); scale bar, 200μm. (D) Quantification of angiogenic sprouts. The number of angiogenic sprouts in the vascular front was measured by dividing the number of angiogenic sprouts by the total length of vascular front (See Supplemental methods for detail). While the number of angiogenic sprouts in the vascular front was mildly decreased by 20% to in P5 *Alk2$^{fl/fl}$* retinas (8.8±0.2 compared to 10.8±1.9 in wildtype littermates), it was decreased by 45% in 14 Bmpr2fl/fl (6.5±1.3 in *Bmpr2$^{fl/fl}$* retinas compared to 11.8±1.6 in wildtype littermates), and by 53% in *Alk3$^{fl/fl}$* retinas (5.3±0.4 in *Alk3$^{fl/fl}$* retinas compared to 11.2±0.9 in wildtype littermates). P<0.05. Statistical significance was assessed using a Student's unpaired t-test.
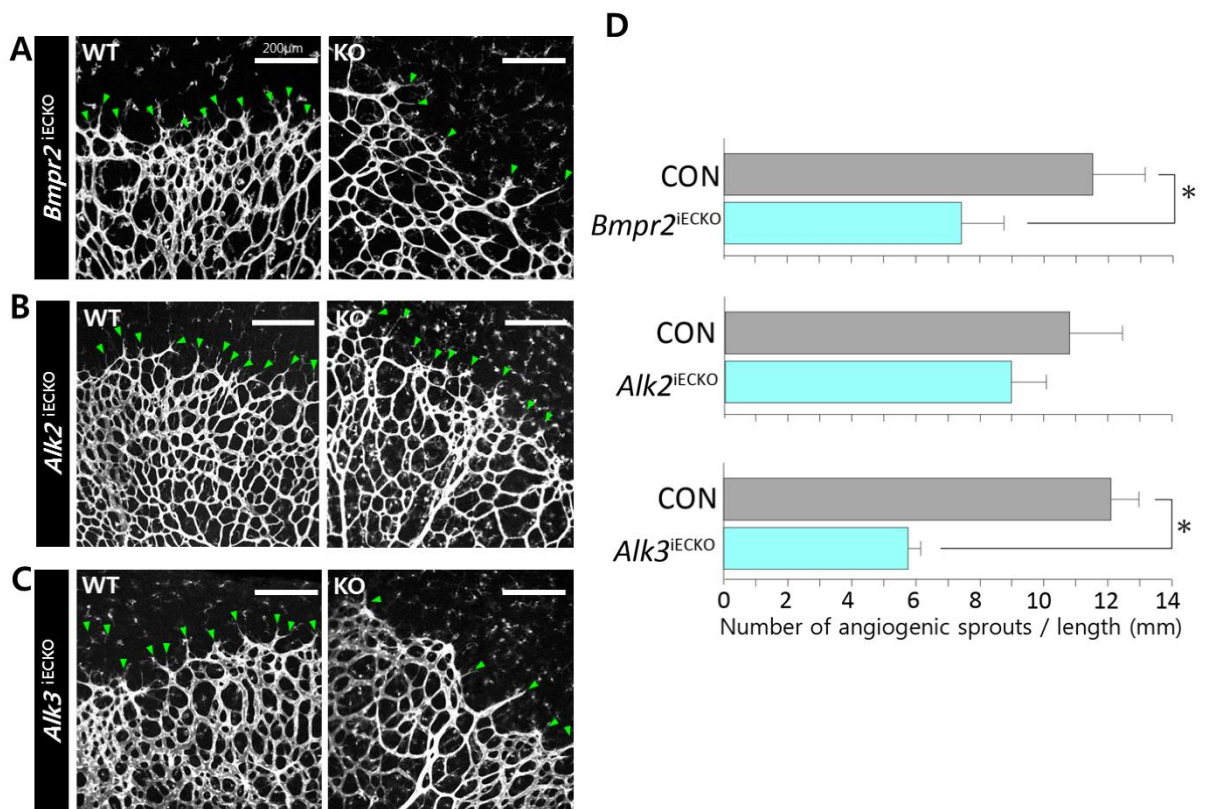
Supplementary Figure 2.1. Expression of BMP ligands in retina during development

Expression of key BMP ligands and VEGF-A in developing mice retinas over time, measured by qRTPCR. Results from biological triplicates are shown.
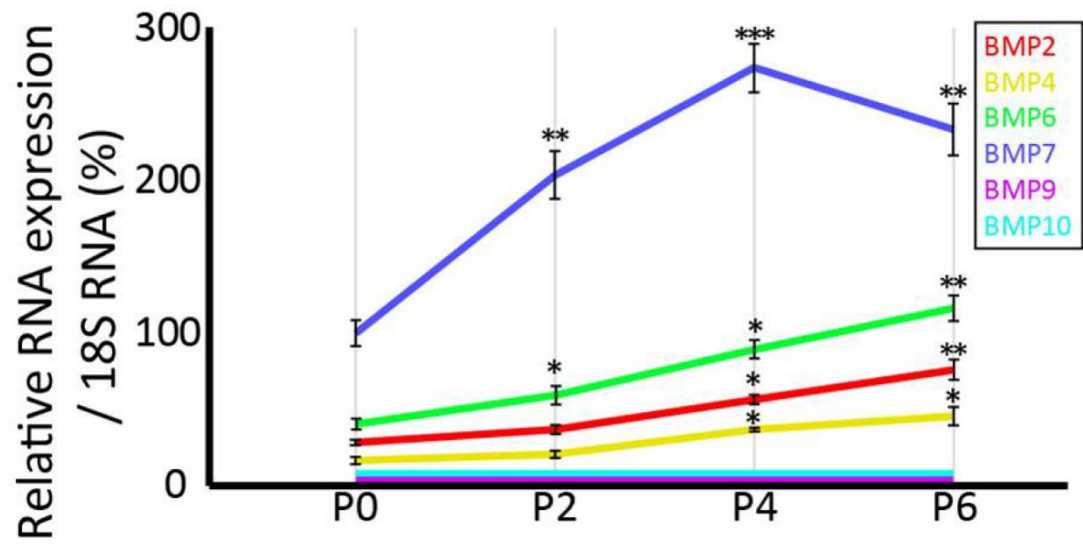
Supplementary Figure 2.2. Expression of BMP ligands in retinal angiogenesis

Expression of BMP ligands which appear to be highly expressed in the retina during P1 to P6

was examined by semi-quantitative RT-PCR (A) and *in situ hybridization* (B).

A

500bp
400bp
300bp
200bp
100bp

BMP2 BMP4 BMP6 BMP7

HUVEC cDNA
PCR

B

| BMP2 | BMP4 | BMP6 | BMP7 |

IB4

BMPs
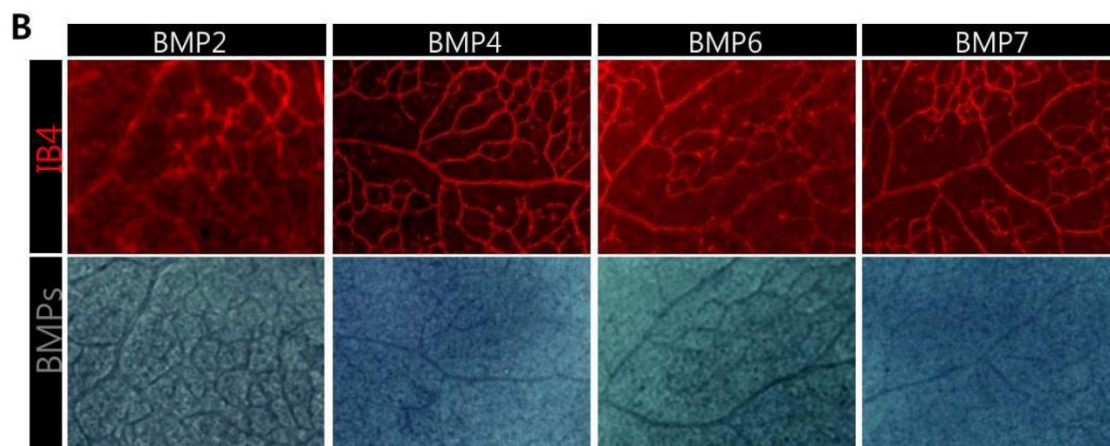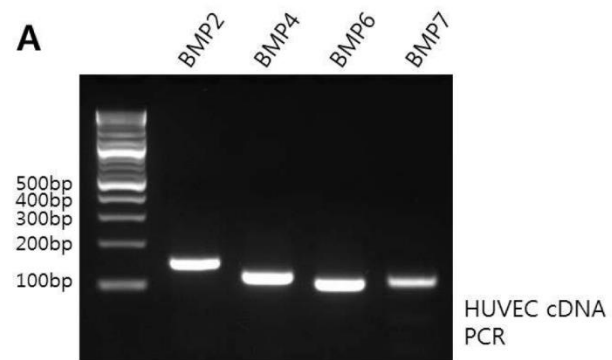
Supplementary Figure 2.3. Expression of BMP receptors in endothelial cells

Expression of BMP receptors in endothelial cells isolated from mice, measured by qRT-PCR

(A) and semi-quantitative PCR (B). Results from biological triplicates are shown.
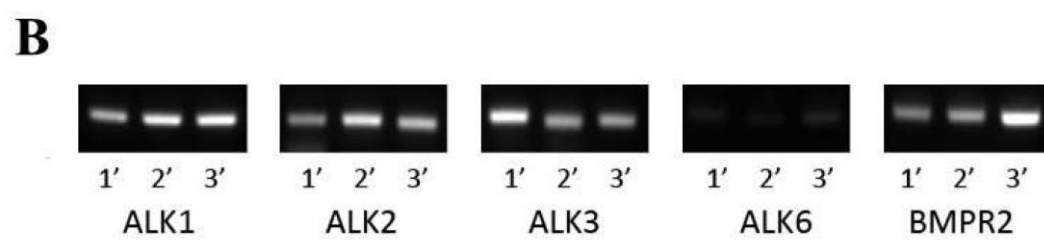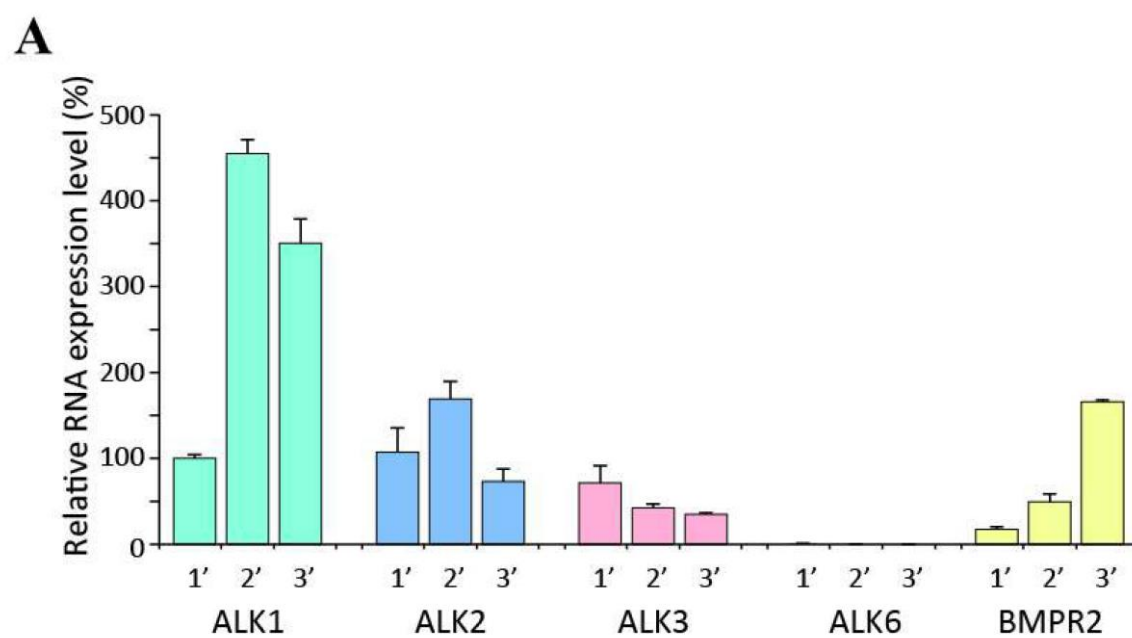
Supplementary Figure 2.4. Deletion efficacy of *Alk2^{fl/fl}* and *Alk3^{fl/fl}*
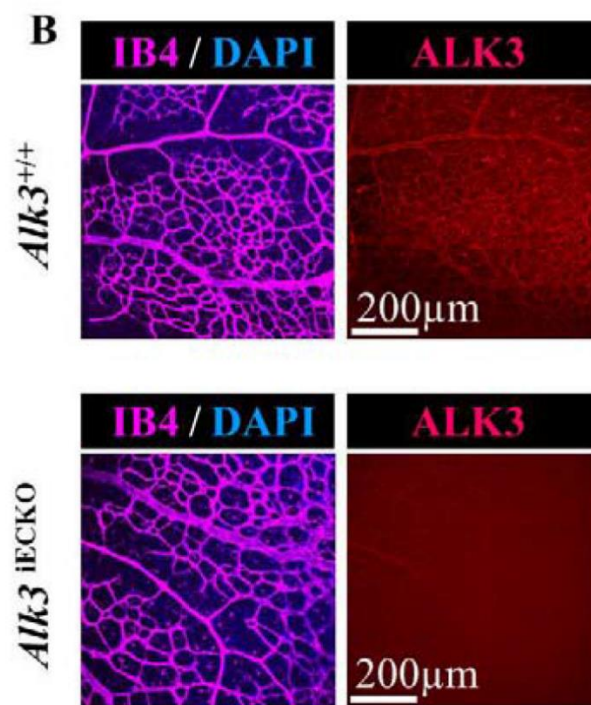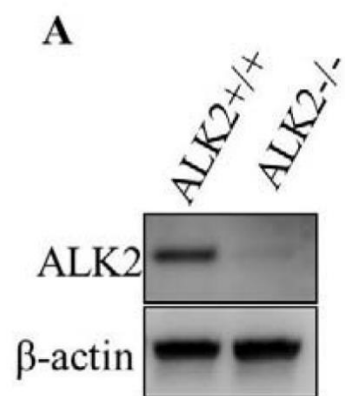
Deletion efficacy of *Alk2* and *Alk3* upon tamoxifen administration was examined by western

(in case of *Alk2*; A) or immunohistochemistry (in case of *Alk3*; B).

REFERENCES

1.   Cai J, Pardali E, Sanchez-Duffhues G, ten Dijke P. BMP signaling in vascular diseases. FEBS Lett. 2012;586(14):1993-2002.

2.   David L, Feige JJ, Bailly S. Emerging role of bone morphogenetic proteins in angiogenesis. Cytokine Growth Factor Rev. 2009;20(3):203-212.

3.   Langenfeld EM, Langenfeld J. Bone morphogenetic protein-2 stimulates angiogenesis in developing tumors. Mol Cancer Res. 2004;2(3):141-149.

4.   Pi X, Ren R, Kelley R, Zhang C, Moser M, Bohil AB, et al. Sequential roles for myosin-X in BMP6-dependent filopodial extension, migration, and activation of BMP receptors. The Journal of Cell Biology. 2007;179(7):1569-1582.

5.   Wiley DM, Kim J-D, Hao J, Hong CC, Bautch VL, Jin S-W. Distinct Signaling Pathways Regulate Sprouting Angiogenesis from the Dorsal Aorta and Axial Vein. Nature cell biology. 2011;13(6):686-692.

6.   Wakayama Y, Fukuhara S, Ando K, Matsuda M, Mochizuki N. Cdc42 mediates Bmp-induced sprouting angiogenesis through Fmnl3-driven assembly of endothelial filopodia in zebrafish. Dev Cell. 2015;32(1):109-122.

7.   Ren R, Charles PC, Zhang C, Wu Y, Wang H, Patterson C. Gene expression profiles identify a role for cyclooxygenase 2-dependent prostanoid generation in BMP6-induced angiogenic responses. Blood. 2007;109(7):2847-2853.

8.   David L, Mallet C, Mazerbourg S, Feige JJ, Bailly S. Identification of BMP9 and BMP10 as functional activators of the orphan activin receptor-like kinase 1 (ALK1) in endothelial cells. Blood. 2007;109(5):1953-1961.

9.   Larrivee B, Prahst C, Gordon E, del Toro R, Mathivet T, Duarte A, et al. ALK1 signaling inhibits angiogenesis by cooperating with the Notch pathway. Dev Cell. 2012;22(3):489-500.

10.   Ricard N, Ciais D, Levet S, Subileau M, Mallet C, Zimmers TA, et al. BMP9 and BMP10 are critical for postnatal retinal vascular remodeling. Blood. 2012;119(25):6162-6171.

11.   Kim J, Kim M, Jeong Y, Lee WB, Park H, Kwon JY, et al. BMP9 Induces Cord Blood-Derived Endothelial Progenitor Cell Differentiation and Ischemic Neovascularization via ALK1. Arterioscler Thromb Vasc Biol. 2015;35(9):2020-2031.

12.   Pouliot F, Blais A, Labrie C. Overexpression of a dominant negative type II bone morphogenetic protein receptor inhibits the growth of human breast cancer cells. Cancer Res. 2003;63(2):277-281.

13.   Townson SA, Martinez-Hackert E, Greppi C, Lowden P, Sako D, Liu J, et al. Specificity and structure of a high affinity activin receptor-like kinase 1 (ALK1) signaling complex. J Biol Chem. 2012;287(33):27313-27325.

14.   Manning G, Whyte DB, Martinez R, Hunter T, Sudarsanam S. The protein kinase complement of the human genome. Science. 2002;298(5600):1912-1934.

15.   Mazerbourg S, Sangkuhl K, Luo CW, Sudo S, Klein C, Hsueh AJ. Identification of receptors and signaling pathways for orphan bone morphogenetic protein/growth differentiation factor ligands based on genomic analyses. J Biol Chem. 2005;280(37):32122-32132.

16.   Aspalter IM, Gordon E, Dubrac A, Ragab A, Narloch J, Vizan P, et al. Alk1 and Alk5 inhibition by Nrp1 controls vascular sprouting downstream of Notch. Nat Commun. 2015;6:7264.

17.   Zhu Q, Kim YH, Wang D, Oh SP, Luo K. SnoN facilitates ALK1-Smad1/5 signaling during embryonic angiogenesis. J Cell Biol. 2013;202(6):937-950.

18.   ten Dijke P, Yamashita H, Sampath TK, Reddi AH, Estevez M, Riddle DL, et al. Identification of type I receptors for osteogenic protein-1 and bone morphogenetic protein-4. J Biol Chem. 1994;269(25):16985-16988.

19.   Komatsu Y, Scott G, Nagy A, Kaartinen V, Mishina Y. BMP type I receptor ALK2 is essential for proper patterning at late gastrulation during mouse embryogenesis. Dev Dyn. 2007;236(2):512-517.

20.   Gu Z, Reynolds EM, Song J, Lei H, Feijen A, Yu L, et al. The type I serine/threonine kinase receptor ActRIA (ALK2) is required for gastrulation of the mouse embryo. Development. 1999;126(11):2551-2561.

21.   Mishina Y, Crombie R, Bradley A, Behringer RR. Multiple roles for activin-like kinase-2 signaling during mouse embryogenesis. Dev Biol. 1999;213(2):314-326.

22.   Mishina Y, Suzuki A, Ueno N, Behringer RR. Bmpr encodes a type I bone morphogenetic protein receptor that is essential for gastrulation during mouse embryogenesis. Genes Dev. 1995;9(24):3027-3037.

23.   Song L, Fassler R, Mishina Y, Jiao K, Baldwin HS. Essential functions of Alk3 during AV cushion morphogenesis in mouse embryonic hearts. Dev Biol. 2007;301(1):276-286.

24.   Wang J, Sridurongrit S, Dudas M, Thomas P, Nagy A, Schneider MD, et al. Atrioventricular cushion transformation is mediated by ALK2 in the developing mouse heart. Dev Biol. 2005;286(1):299-310.

25. Tual-Chalot S, Mahmoud M, Allinson KR, Redgrave RE, Zhai Z, Oh SP, et al. Endothelial depletion of Acvrl1 in mice leads to arteriovenous malformations associated with reduced endoglin expression. PLoS One. 2014;9(6):e98646.

26. Kaartinen V, Dudas M, Nagy A, Sridurongrit S, Lu MM, Epstein JA. Cardiac outflow tract defects in mice lacking ALK2 in neural crest cells. Development. 2004;131(14):3481-3490.

27. Mishina Y, Hanks MC, Miura S, Tallquist MD, Behringer RR. Generation of Bmpr/Alk3 conditional knockout mice. Genesis. 2002;32(2):69-72.

28. Beppu H, Lei H, Bloch KD, Li E. Generation of a floxed allele of the mouse BMP type II receptor gene. Genesis. 2005;41(3):133-137.

29. Benedito R, Roca C, Sorensen I, Adams S, Gossler A, Fruttiger M, et al. The notch ligands Dll4 and Jagged1 have opposing effects on angiogenesis. Cell. 2009;137(6):1124-1135.

30. Moya IM, Umans L, Maas E, Pereira PN, Beets K, Francis A, et al. Stalk cell phenotype depends on integration of Notch and Smad1/5 signaling cascades. Dev Cell. 2012;22(3):501-514.

31. Magee JC, Stone AE, Oldham KT, Guice KS. Isolation, culture, and characterization of rat lung microvascular endothelial cells. American Journal of Physiology - Lung Cellular and Molecular Physiology. 1994;267(4):L433-L441.

32. Sakurai E, Sakurada T, Ochiai Y, Yamakami J, Tanaka Y. Stereoselective transport of histidine in rat lung microvascular endothelial cells. American Journal of Physiology - Lung Cellular and Molecular Physiology. 2002;282(6):L1192-L1197.

33. Powner MB, Vevis K, McKenzie JA, Gandhi P, Jadeja S, Fruttiger M. Visualization of gene expression in whole mouse retina by in situ hybridization. Nat Protoc. 2012;7(6):1086-1096.

34. Monteiro RM, de Sousa Lopes SM, Bialecka M, de Boer S, Zwijsen A, Mummery CL. Real time monitoring of BMP Smads transcriptional activity during mouse development. Genesis. 2008;46(7):335-346.

35. Little SC, Mullins MC. Bone morphogenetic protein heterodimers assemble heteromeric type I receptor complexes to pattern the dorsoventral axis. Nat Cell Biol. 2009;11(5):637-643.

36. Luo J, Tang M, Huang J, He BC, Gao JL, Chen L, et al. TGFbeta/BMP type I receptors ALK1 and ALK2 are essential for BMP9-induced osteogenic signaling in mesenchymal stem cells. J Biol Chem. 2010;285(38):29588-29598.

37.	Scharpfenecker M, van Dinther M, Liu Z, van Bezooijen RL, Zhao Q, Pukac L, et al. BMP-9 signals via ALK1 and inhibits bFGF-induced endothelial cell proliferation and VEGF-stimulated angiogenesis. J Cell Sci. 2007;120(Pt 6):964-972.

Chapter 3: Tortuous Microvessels Contribute to Wound Healing via Sprouting Angiogenesis[2]

3.1 Summary

Wound healing is accompanied by neoangiogenesis, and new vessels are thought to originate primarily from the microcirculation; however, how these vessels form and resolve during wound healing is poorly understood. Here, we investigated properties of the smallest capillaries during wound healing to determine their spatial organization and the kinetics of formation and resolution. We utilized intravital imaging and high-resolution microscopy to identify a new type of vessel in wounds, called tortuous microvessels. Longitudinal studies showed that tortuous microvessels increased in frequency after injury, "normalized" as the wound healed, and were closely associated with the wound site. Tortuous microvessels had aberrant cell shapes and distinct interactions with circulating microspheres, suggesting altered flow dynamics. Moreover, tortuous microvessels disproportionately contributed to wound angiogenesis by sprouting exuberantly and significantly more frequently than nearby normal capillaries. A new type of transient wound vessel, tortuous microvessels, sprout dynamically and disproportionately contribute to wound healing neoangiogenesis, likely as a result of altered properties downstream of flow disturbances. These new findings suggest entry points for therapeutic intervention.

3.2 Introduction

Angiogenesis, the formation of new blood vessels via sprouting, is a complex process whereby endothelial cells migrate out from pre-existing vessels and form new connections to increase the vascular network [1-5]. During development, angiogenesis occurs in response to tissue cues such as hypoxia and is critical for proper growth of the embryo [5-7]. In contrast, endothelial cells are largely quiescent in adults; however, they become activated to reinitiate angiogenesis in physiological processes such as wound healing or in diseases such as cancer [8]. Unlike developmental angiogenesis, physiological angiogenesis is often characterized by the formation of tortuous vessels [9-12]. Tortuous vessels have a distinct morphology, displaying S-shaped curves, oscillations, or kinks compared to normal linear vessels, and they are often excessively permeable [13]. Although tortuous vessels have been observed for decades, it is not clear how these vessels form, how they contribute to angiogenesis, or how they resolve.

Wound healing is characterized by several phases [14-16], including a proliferative phase in which angiogenesis is a major component. Tortuous vessels often appear during the proliferative phase, and their occurrence decreases as the wound heals [17]. Tortuous vessels are thought to result from increased cytokine and growth factor signaling, changes in flow dynamics, changes in extracellular matrix composition, and/or decreased mural cell coverage [9, 13]. Tortuous vessels also have increased permeability [18], which may facilitate delivery to the wound site. Tortuous vessels associated with wound healing have been examined at the macro level via immunohistochemistry and intravital imaging [13, 17, 19, 20], but it is unclear whether tortuosity extends to the smallest capillaries that are the source of most

wound-healing angiogenesis, and the cellular parameters associated with formation and resolution of vessel tortuosity are poorly understood.

Here, we use intravital imaging to analyze the role of tortuous capillary vessels, called tortuous microvessels, during wound healing. Longitudinal analysis of healing in the mouse ear allowed for capture of vessel dynamics over time. Similar to larger vessels, tortuous microvessel frequency increased and then gradually decreased relative to normal capillaries in the wound site. High-resolution imaging *in vivo* revealed that endothelial cells comprising tortuous microvessels have aberrant cell shapes and suggest altered flow dynamics. Surprisingly, tortuous microvessels have increased sprouting compared to normal capillaries, indicating for the first time that tortuous vessels contribute to sprouting angiogenesis during wound healing. Thus, we identify a new type of tortuous vessel that forms from the smallest capillaries and contributes significantly to sprouting angiogenesis in wounds. Due to its exuberant sprouting, this class of vessel may be a novel interventional target for improved wound healing.

3.3 Material and Methods

Mouse Strains

All experiments involving animals were performed with approval of the University of North Carolina, Chapel Hill Institutional Animal Care and Use Committee. Flk1-GFP mice [*Kdr^{tm2.1Jrt}/J*, JAX #017006] express GFP in endothelial cells as previously described [21]. R26R tdTomato [*Gt(ROSA)26Sor^{tm14(CAG-tdTomato)Hze}/J*, JAX #007914] mice have a STOP cassette flanked by *loxP* sites followed by tdTomato [22]. Cdh5(PAC)-CreERT2 transgenic

mice were generated by microinjecting a transgene containing a genomic Cdh5(PAC) promoter fragment fused to a CreERT2 cDNA into zygotes [23]. Cre was induced by one application (7 days prior to biopsy punch) of a 10nM solution of tamoxifen dissolved in DMSO to the mouse ear for 10 min, then rinsing with ethanol.

Intravital Imaging

Flk1-GFP mice were commercially obtained from Jackson Laboratory and bred into a CD1 background. Mice were anesthetized using 2% isoflurane and a 0.35mm biopsy punch (Fine Science Tools) was used to create a small wound. To perform intravital imaging, we adhered to a protocol established by Chan et al. [24]. Briefly, mice were placed in an induction chamber, anesthetized with 3-4% isoflurane, and then placed on a heating pad with continuous 2% isoflurane inhalation. Multiphoton imaging was performed on an Olympus FV1000MPE microscope mounted on an upright BX-61WI microscope, using a 25x objective, with a custom-built aluminum clamp to immobilize the ear during imaging. A coupling gel composed of 300 mM D-sorbitol (Sigma-Aldrich) and 0.5% Carbomer 940 (Spectrum Chemical) adjusted to pH 7.4, was placed between the objective and coverslip. We used a 910nm excitation wavelength to image GFP, and a 960nm excitation wavelength to simultaneously image GFP and tdTomato. Images were obtained using the Multi Area Time Lapse tool on the Olympus Fluoview software in a 5x5 grid (~1.5mm x 1.5mm) of the wound and the surrounding area. Images were processed using Fiji and were stitched together using the Grid/Stitching Plugin.

Tortuosity Index

To calculate tortuosity index, a modified equation from Bullitt et al. [25] was used. We measured the ratio between the shortest distance of the start and end point of a vessel segment, noted as the geodesic distance (L_G), over the total distance of a vessel segment, noted as Euclidian distance (L_E). We then multiplied this ratio by the number of inflection points, or the number of times the vessel changes direction with a degree of $< 160^0$ (N_C). Statistical significance was quantified using GraphPad Prism software and an unpaired t-test where $p<0.05$ was significant. To determine the cut-off value for tortuosity, a receiver operating characteristic (ROC) curve was used to calculate 3.2 as the value where there is 100% specificity and 94% sensitivity

In Vivo Flow Experiments

To visualize *in vivo* blood flow, we injected 0.1 µm, red fluorescent, FluoSpheres® Carboxylate-Modified Microspheres (Invitrogen). Mice were anesthetized with 3% isoflurane and a tail vein catheter was used to administer a solution of 10% microspheres in sterile PBS. To simultaneously image GFP and red spheres, an excitation wavelength of 960nm was used. For live capture, we imaged using an Olympus FV1000MPE microscope and acquired images at frame rate of 1.1 frames/sec using a 25x objective. Images were processed using Fiji.

Antibody Staining

Mice were euthanized and perfused with 4% PFA. Ears were removed and dissected to expose vessels and fixed an additional 2 hr with 4% PFA. Tissue was then rinsed with PBS, permeabilized with a 1% Triton X-100/PBS solution for 1hr, then blocked overnight

with 5% Serum/0.5% Triton X-100/1% BSA/ PBS (blocking solution). Tissue was incubated

with PECAM antibody (BD Biosciences) in blocking solution at a 1:100 dilution, overnight

at 4^0C. The samples were rinsed with PBS, incubated with Alexa-Fluor 555 secondary

antibody for 2hr, then rinsed with PBS and mounted onto slides using Vectashield Hard Set

Mounting Media (Vectashield). Images were acquired on an Olympus FV1200 using a 40x

objective and processed using Fiji.

Vessel Length and Sprout Analysis

Vessels segments were traced and isolated using a mask function in Fiji. Tracings

were skeletonized using the skeletonize plugin in Fiji and analyzed using the Analyze

Skeleton Plugin in Fiji. Total traced segments were used to determine the percentages of

tortuous microvessels and normal capillaries for each time point. For sprouting, images were

stacked to make a time series. The Cell Counter Plugin was used to annotate sprout

initiations, connections, and retractions from normal and tortuous sprouts. Significance was

determined using Two-Way ANOVA, with $p \leq 0.05$ being significant.

3.4 Results

Tortuous Microvessels Are Associated with Wound Healing

To better understand the role of angiogenesis in wound healing, we investigated this

process in a mouse ear wound healing model. We employed a *Flk1*-GFP vascular reporter

line [21] and a small ear punch biopsy (0.35mm) to induce a wound, and we examined

angiogenesis and tortuous vessel formation as the wound healed. Using intravital imaging

and two-photon microscopy, we acquired high-resolution images (including the Z-plane) of

small caliber vessels growing into the wound site of the same mouse ear over an extended

time period (up to 39 days post wounding, dpw) **(Figure 3.1A-C; Supplementary Figure 3.1)**. Image analysis revealed that small caliber tortuous vessels, which we termed tortuous microvessels, were present in the wound area as early as 3dpw, alongside normal small capillaries **(Figure 3.1D-I)**.

We defined a tortuous microvessel as having a diameter of 5-20 µm and oscillating S-curves, kinks, bends, or twists. To accurately quantify tortuous microvessels during wound healing, we applied a tortuosity index (TI) to vessel segments and found that TI values for tortuous microvessels were significantly higher than those for normal nearby microvessels in the wound, verifying that this vessel type has a distinct morphology that can be quantified **(Supplementary Figure 3.2A-C)**. Tracing and binning of all microvessels in the images revealed that the total length of microvessels significantly increased from 3dpw to 17dpw, coinciding with the angiogenic phase of wound healing, then leveled off during subsequent times **(Supplementary Figure 3.2D)**. The percentage of tortuous microvessels also followed this time course initially and peaked at 17dpw; however, tortuous microvessels then significantly decreased as healing progressed **(Figure 3.1J)**. Comparison of start, peak, and end points showed that the percentage increase in tortuous microvessels was significant at 17dpw compared to the beginning and end of the imaging time **(Figure 3.1K)**. Thus tortuous microvessel formation increased initially as part of the overall trend, but then decreased while overall microvessel length stabilized, suggesting that tortuous microvessels resolve into normal capillaries over time.

To more closely examine the relationship between tortuous microvessels and wound closure, we measured microvessel location relative to the wound. Circular regions were outlined every 100 µm outward from the wound center and used to calculate the percentage

of tortuous microvessels in these regions at each time point **(Figure 3.2A).** We found that the majority of vessels near the wound boundary (100-300 μm from centroid) were tortuous **(Figure 3.2B)**. Because most tortuous microvessels were found close to the wound boundary, we next asked how tortuous microvessels formed in new tissue that is initially avascular. We outlined the avascular area (including the biopsy punch hole) around the wound at 1dpw, and used this constant area to assess new angiogenesis at subsequent time points **(Figure 3.2C, Supplementary Figure 3.3A-B)**. The area remained avascular until 5dpw, and subsequent vascularization consisted mainly of tortuous microvessels at early time points (7-17dpw) **(Figure 3.2D)**. However, as the wound remodeled, the total length of the tortuous microvessels decreased while the total length of the normal capillaries in this area increased, and the two lengths were equal by 31-39 dpw. To determine if the predominant vascularization by tortuous microvessels at the early time points was due to angiogenesis, tissue migration into the wound area, or a combination of both, we tracked the location of distinct vessels in this region over time. We found that the wound area initially showed some mass movement, suggesting that microvessels may move in due to larger tissue displacement at early time points **(Supplementary Figure 3.3)**. However, we tracked individual patterns over time and found that, starting around 7-9dpw, mass movement was minimal and new microvessels appeared to form via sprouting angiogenesis into the avascular region **(Supplementary Figure 3.3B)**. These findings suggest that sprouting angiogenesis is the driving force behind vascularization of new tissue after a short burst of tissue displacement, and that sprouting angiogenesis is active at the wound border where tortuous microvessels are concentrated.

We next hypothesized that the shift from tortuous to normal microvessels in the avascular area resulted at least in part from resolution of tortuous vessels, and we temporally tracked individual tortuous microvessels over time to test this hypothesis **(Figure 3.2E-F).** We found that 69% of tortuous microvessels normalized, while 27% of microvessels remained tortuous over the time course of wound healing, suggesting that tortuous microvessel formation and resolution is a dynamic process associated with the angiogenic phase of wound healing.

Tortuous Microvessel Endothelial Cells have Distinct Properties

We took advantage of high-resolution intravital imaging to interrogate the endothelial cells that line tortuous microvessels. The topology of tortuous microvessels suggested that, similar to larger tortuous vessels, they experience disturbed flow, and as a result, the endothelial cells may change shape and acquire other properties consistent with a state of "activation" [26]. We acquired images from live intravital imaging while injecting small-diameter fluorescent microspheres to visualize blood flow. Before injection, there were no red fluorescent microspheres present in any vessels **(Figure 3.3A)**. Upon injection, the microspheres moved through the imaging field quickly in areas with linear capillaries, and microsphere patterns changed completely from one time frame to the next **(Figure 3.3B-F,** blue boxes**)**. In contrast, some microspheres appeared to "stick" in the curved area of tortuous microvessels, and these became more prevalent with time **(Figure 3.3B-G,** red boxes**)**, while the linear regions lost association with microspheres over time as they were presumably cleared from the circulation. Analysis revealed that on average 5 beads per tortuous microvessel remained stationary post-injection, while no beads were stationary in linear microvessels **(Figure 3.3H)**. These findings indicate that endothelial cells in tortuous

microvessels differ from those in linear regions, and suggest that reduced or disturbed blood flow is associated with tortuous microvessels, which could ultimately lead to differences in endothelial cell properties between normal and tortuous microvessels.

Since activated endothelial cells are often round rather than being spindle-shaped and elongated, we hypothesized that endothelial cells in tortuous microvessels had abnormal cell shapes. To test this hypothesis, we generated mosaic mouse lines that expressed GFP in endothelial cells along with a vascular-selective inducible Cre driver, *Cdh5*-CreERT2 [23], and a tdTomato excision reporter [22]. The reporter was activated in a small subset of endothelial cells (10-30%) using low-dose tamoxifen prior to wound healing, and individual groups of endothelial cells were followed over the wound healing time course. Endothelial cells in normal capillaries maintained a stereotypical spindle shape, while those in tortuous microvessels were spindle-shaped at 1dpw, but became more rounded over time, coincident with increased tortuosity **(Figure 3.4A-B)**. The shapes of individual endothelial cells were measured at 11dpw in fixed samples stained for PECAM-1, an endothelial cell border marker **(Figure 3.4C)**. The longitudinal/transverse axis ratio was significantly reduced in endothelial cells from tortuous microvessels relative to control endothelial cells in normal microvessels **(Figure 3.4D)**. These data confirm the visual appearance of endothelial cells in tortuous microvessels as rounded and suggestive of "activation". Taken together, these results show that endothelial cells in tortuous microvessels behave abnormally by several criteria.

Tortuous Microvessels Sprout Robustly

The altered morphology and properties of tortuous microvessel endothelial cells suggest that they are more "activated" than endothelial cells in normal capillaries, and activation is often associated with sprouting. Thus we hypothesized that tortuous microvessel

endothelial cells sprout more frequently than normal capillaries, and we used our high-resolution longitudinal dataset of wound healing angiogenesis to test this idea. Analysis of blood vessel sprouts, defined as new extensions of at least 10µm that were unconnected (blind-ended) and that initiated during the wound healing time course, revealed that tortuous microvessels sprouted exuberantly **(Figure 3.5A-G)**. For example, a microvessel near the wound that appeared normal at 1dpw subsequently became tortuous at 5dpw, and sprouts emanated from curved regions **(Figure 3.5A-B)**. At 7dpw, the main microvessel remained tortuous, and the sprouts continued to extend **(Figure 3.5C)**. By 9dpw onward, the main microvessel began to normalize, while the sprouts persisted and made connections to each other or to other vessels **(Figure 3.5D-F)**. When analyzing new sprout initiations, we found that tortuous microvessels sprouted at a significantly higher frequency than normal capillaries from 5-13dpw **(Figure 3.5G)**.

To determine if sprout initiations from tortuous microvessels were more or less stable than sprout initiations from normal vessels, we quantified how often sprouts from each type of vessel formed a connection or retraction **(Supplementary Figure 3.4A-B)**. Our analysis showed no significant differences between connections and retractions of sprouts from tortuous or normal microvessels **(Supplementary Figure 3.4C)**, suggesting that sprouting from tortuous vessels leads to stable connections and expand the vascular plexus near the wound site. We asked whether sprouting from tortuous microvessels was a resolution mechanism, and found that 36% of tortuous microvessels normalized after sprouting while 54% normalized without sprouting, suggesting that sprouting is not required for vessel normalization **(Supplementary Figure 3.4D)**.

To better understand the sprouting behavior of tortuous microvessels, we examined when sprout initiations occurred relative to acquisition of microvessel tortuosity (**Figure 3.5H-L**). This analysis showed that significantly more sprouts formed after microvessels became tortuous compared to sprouts initiating co-incident with tortuosity (**Figure 3.5L**), suggesting that sprouting is downstream of tortuous vessel formation. This data suggests that endothelial cells remain inactive and less likely to sprout absent tortuosity. To determine if there were regions within tortuous microvessels that were more "active," we measured sprout initiations from curved regions vs. non-curved regions of tortuous microvessels. Our data revealed a significant increase in sprout frequency from the apex of the curved region of tortuous microvessels vs. other areas of the vessel (**Figure 3.5M-O**), suggesting that these curved areas are the most active regions of tortuous microvessels. Taken together, these data support our hypothesis that endothelial cells in tortuous microvessels are distinct and perhaps activated, and the enhanced sprouting frequency combined with enhanced overall tortuosity suggest that tortuous microvessel formation is a key player during the angiogenic phase of wound healing.

3.5 Discussion

Here we identify tortuous microvessels for the first time, and present a longitudinal, in-depth analysis of microvessel tortuosity during wound healing. Microvessel tortuosity increases over a reproducible time course that largely correlates with increased overall angiogenesis. We show that sprouting is promoted from tortuous microvessels, and this exuberant sprouting likely contributes significantly to wound angiogenesis and overall healing. Our data is consistent with a model whereby tortuosity alters flow parameters and leads to endothelial cell activation that promotes sprouting in these regions (**Figure 3.5P**).

Thus, the emergence of tortuous microvessels near a wound site may be a mechanism to efficiently expand wound angiogenesis and promote healing.

Although tortuous vessels have been observed during wound healing and in diseases such as cancer [13, 27], microvessels of the caliber (5-20um) analyzed here were not resolved by most of these studies. Yet the bulk of the vasculature in most vessel beds is comprised of small caliber capillaries, and these capillaries are usually the source of sprouts that contribute to neo-angiogenesis. While some studies analyzed static images of wound vessels [13, 28, 29], our approach allowed for high spatio-temporal resolution of microvessels and longitudinal analysis of this critical component of wound healing. Our finding that tortuous microvessels contribute significantly to overall sprouting angiogenesis in the wound environment, and our results showing that these sprouts often lead to new connections and conduits, provide a novel link between vessel tortuosity and wound healing via sprouting angiogenesis.

Sprouting from tortuous microvessels occurs at a higher frequency than from normal vessels, and these sprouts often initiate from the apex of curved regions of tortuous microvessels. While we don't have the resolution to interrogate junctional integrity, our finding that microspheres become "stuck" in the tortuous microvessels suggests altered blood flow and shear stress. Interestingly, a recent study by Ghafarri et al. showed that sprouts emanate from the lowest minimum in predicted shear stress along a capillary network, indicating that reduced shear stress promotes sprouting events [30]. Given these results, and our live-capture of circulating microspheres, we predict that shear stress is lower and/or disturbed in tortuous microvessels relative to normal capillaries downstream of altered vessel morphology. The altered shape of endothelial cells within tortuous microvessels is consistent

with this idea, since relative loss of the laminar flow vector is predicted to loosen junctions, "activate" endothelial cells, and promote sprouting. Likewise, the enhanced sprout initiations we observed from the apex of curved regions suggest that altered flow may induce local discontinuities that are optimized for sprouting in those regions.

What triggers tortuous microvessel formation during wound healing? It is likely a complex combination of local environmental cues and other changes associated with wound healing, since the tortuous microvessels resolve over time. The peak frequency of tortuous microvessels roughly corresponds to the "angiogenic phase" of wound healing [14], and it is known that pro-angiogenic cytokines such as VEGF induce tortuosity [15, 27, 31]. Tortuous microvessels are enriched close to the wound border, which is the most hypoxic area of the wound, consistent with pro-angiogenic influences. However, pro-angiogenic signals are not sufficient to induce vessel tortuosity since most developmental angiogenesis occurs independent of tortuosity. Wound healing is also associated with transient inflammation, so pro-inflammatory cytokines may also contribute to microvessel tortuosity. In any case, it is likely that local changes in the wound healing environment promote tortuosity, and this work shows that vessel tortuosity contributes substantially to microvessel sprouting and neo-angiogenesis that promotes wound healing.

The wound healing process is a natural physiological response, but wound healing is compromised in some diseases as a result of defective vascularization. For example, wound healing is often defective in diabetic patients and sometimes results in limb amputation, and a defective angiogenic response from the microcirculation contributes to this dysfunction [32, 33].The microcirculation is comprised of capillaries that make up the bulk of the vasculature and readily respond to signaling cues. Here, we identify a new class of vessel, a tortuous

microvessel, that is associated with wound healing and contributes significant angiogenic sprouting to the process. Knowledge of the contribution of tortuous microvessels to angiogenic sprouting and wound healing will be useful in thinking of new therapeutic approaches to accelerate and improve wound healing.

3.6 Figures

Figure 3.1. Tortuous microvessels during wound healing.

(A-C) Wound and surrounding vasculature at indicated times. Yellow stippled line, wound punch and avascular area; boxes, areas magnified below. (D-F) High magnification of blue boxed areas showing normal microvessels. (G-I) High magnification of red boxed areas showing tortuous microvessels. (J) Quantification of percentage of tortuous microvessels over time, n=3 ears. (K) Graph representing the ratio of tortuous to normal microvessels at indicated times, n= 3 ears. Error bars, mean $\pm$ SEM; Statistical comparisons by Two-Way ANOVA with Tukey's Multiple Comparison Test; *, p$\leq$0.05; ****, p$\leq$0.0005. Scale bars: 200 µm (A), 50 µm (D). Vessels pseudo colored using Photoshop. dpw, days post wounding.

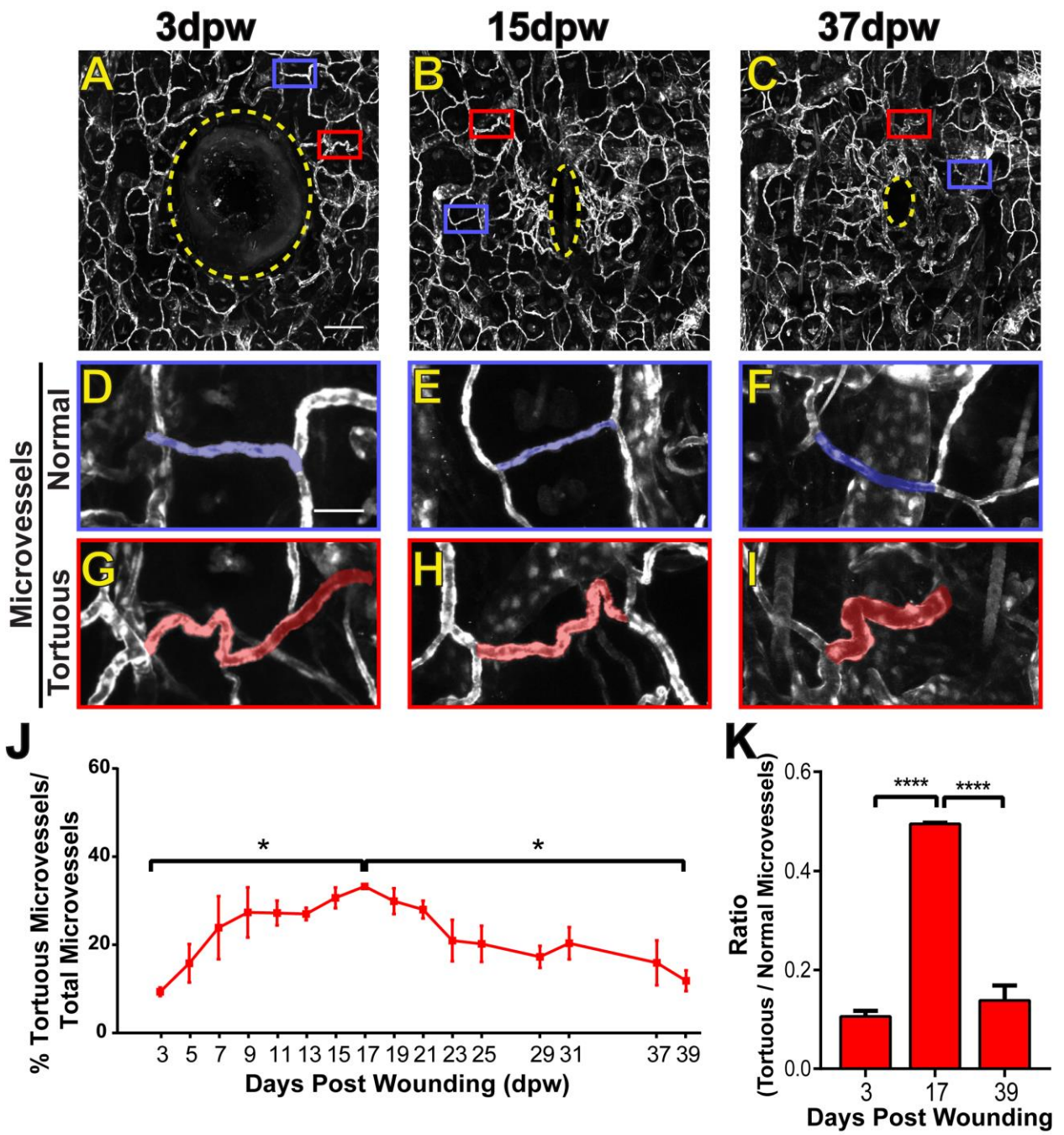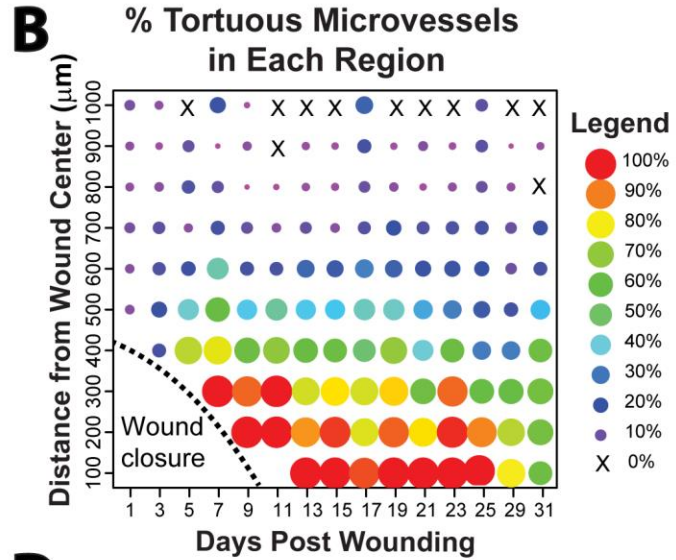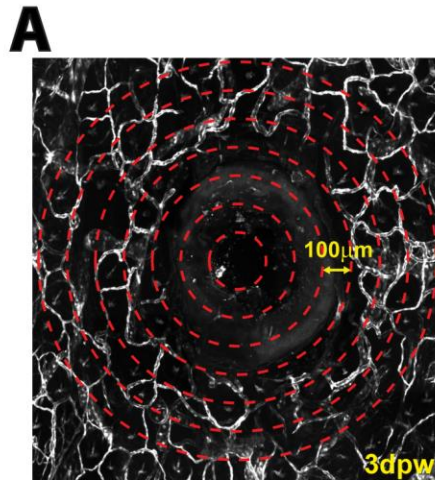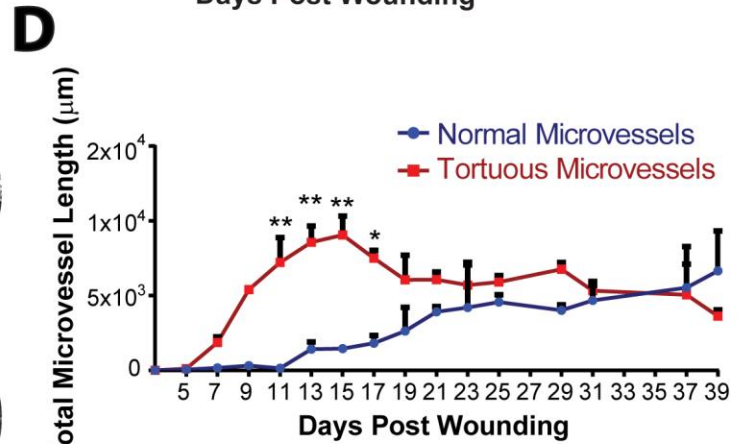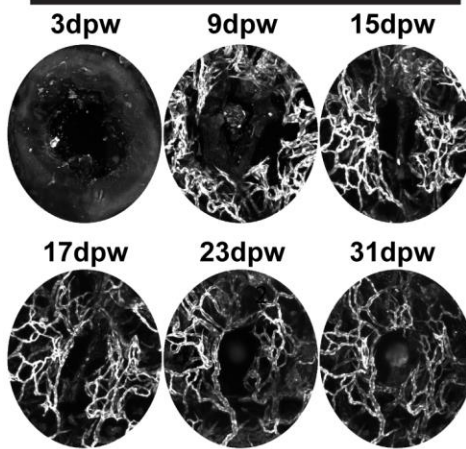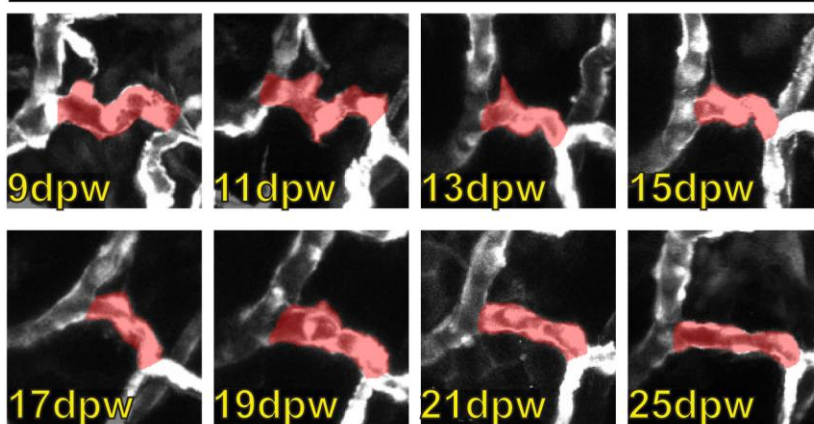**Figure 3.2. Tortuous microvessel location, formation, and resolution.**

(A) Example of 3dpw wound illustrating defined regions every 100 µm (not to scale). Note avascular area (wound punch + tissue) in segments close to the wound. (B) Dot plot representing percentage of tortuous microvessels in each region over time. Warmer colors (red/orange), elevated tortuous microvessels; cooler colors (blue/purple), reduced tortuous microvessels. (C) Avascular wound area + punch, defined at 1dpw and analyzed at subsequent time points. (D) Quantification of normal and tortuous microvessel length in new wound tissue (same areas measured for all time points). Error bars, mean + SEM. Statistical comparisons, Two-Way ANOVA with Sidak's Multiple Comparisons test. *, $p \leq 0.05$, **$p \leq 0.005$. (E) Example of a tortuous microvessel over time, showing normalization. (F) Percentage of vessels that normalized, remained tortuous, or outcome unknown during 39 day wound healing time course. n=86 tortuous microvessels. Vessels pseudo colored using Photoshop. dpw, days post wounding.

A 100μm 3dpw

B % Tortuous Microvessels in Each Region

Distance from Wound Center (μm) vs Days Post Wounding

Wound closure

Legend
- 100% (red)
- 90%
- 80%
- 70%
- 60%
- 50%
- 40%
- 30%
- 20%
- 10%
- X 0%

C Avascular area at 1dpw
3dpw, 9dpw, 15dpw, 17dpw, 23dpw, 31dpw

D Total Microvessel Length (μm) vs Days Post Wounding
- Normal Microvessels
- Tortuous Microvessels
** ** ** *

E Microvessel Normalization
9dpw, 11dpw, 13dpw, 15dpw, 17dpw, 19dpw, 21dpw, 25dpw

F Tortuous Microvessel Resolution
- Normalized 69%
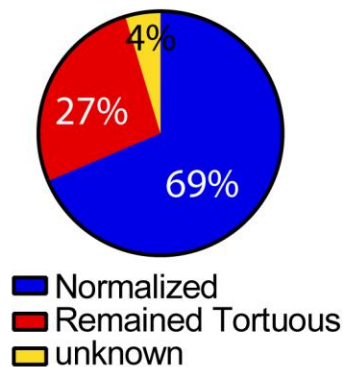- Remained Tortuous 27%
- unknown 4%

77

Figure 3.3. Circulating microspheres accumulate in tortuous microvessels.

Representative images from movie of circulating microspheres; time (T) sec, upper right. (A) Prior to injection of microspheres into tail vein. (B-F) Images post-injection at indicated times. Blue insets, linear microvessel; red insets, tortuous microvessel; yellow arrowheads, microspheres stationary for multiple time frames. Note that no microspheres remain in the normal vessel segment (blue inset) as opposed to trapped microspheres in the tortuous microvessel (arrows in red inset). (G) Illustration showing tortuous microvessel and areas where microspheres became trapped. (H) Quantification of microsphere trapping in normal and tortuous microvessels; long line and error bars, mean +/- SEM. Statistical comparisons, Students t-test (unpaired, two-tailed). *, $p \leq 0.05$. Scale bar, 50 µm.
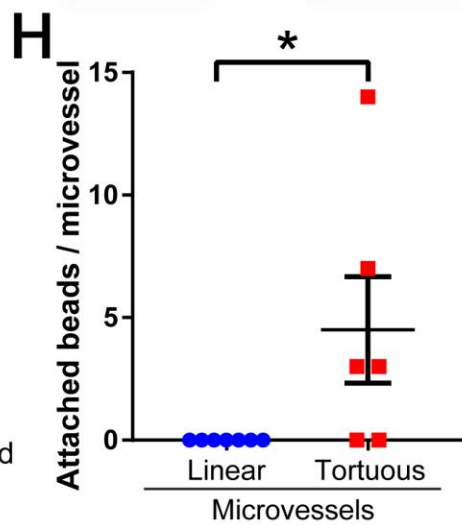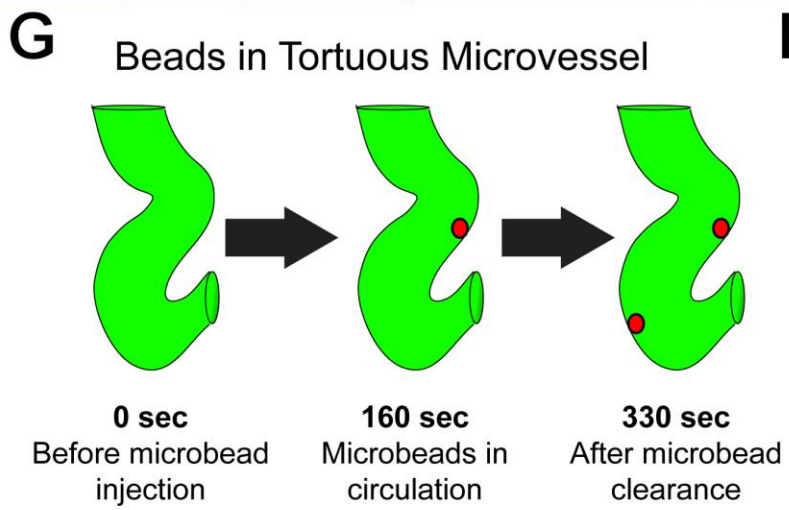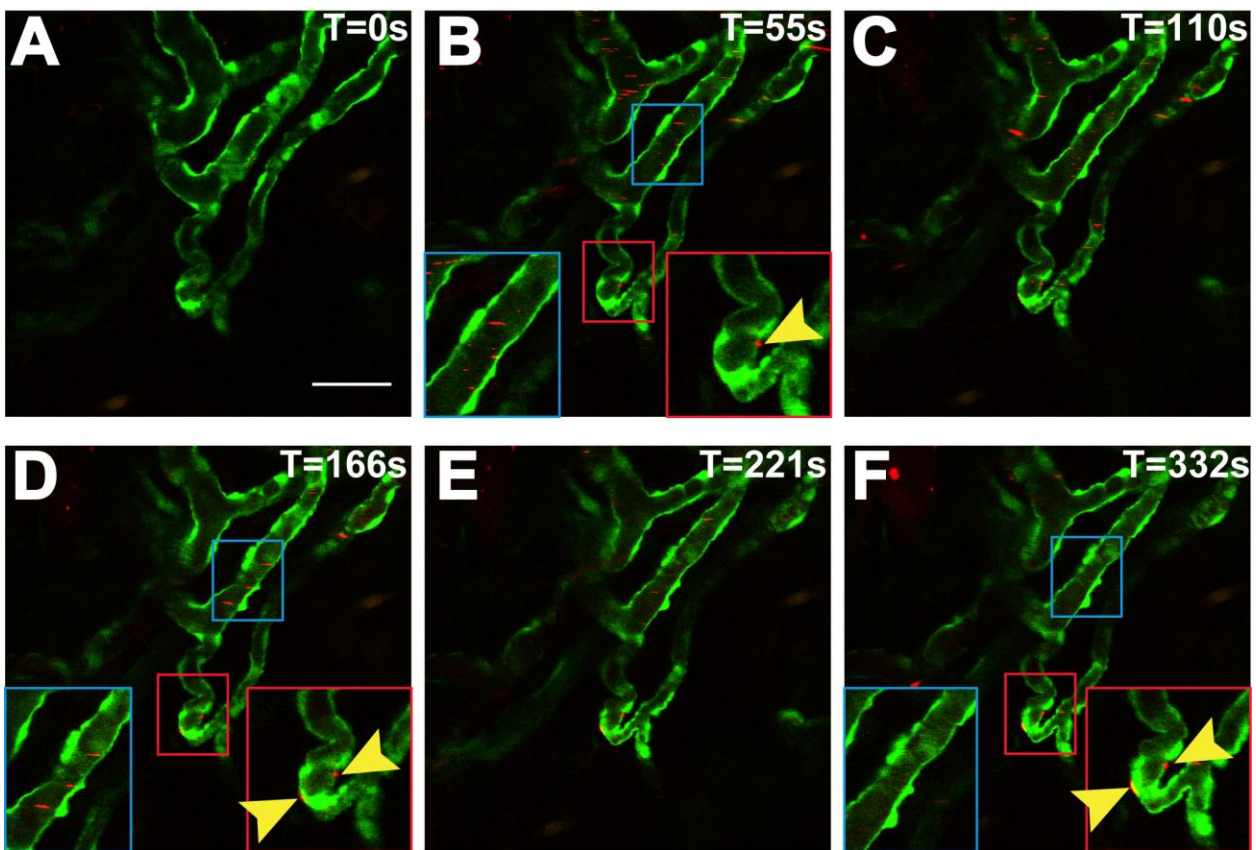
Figure 3.4. Cellular morphology in tortuous microvessels.

Mosaic analysis of microvessels during wound healing in mice of indicated genotype. (A) Normal microvessel EC have stereotypical spindle morphology throughout time course (blue arrowheads, red cell in diagram). (B) Tortuous microvessel EC initiate as spindle-like and become rounded with time and tortuosity (blue arrowheads, red cell in diagram). (C) PECAM staining of Flk1-GFP mice at 11dpw highlighting individual cell borders. (D) Ratio of longitudinal to transverse axis of EC in normal and tortuous microvessels; long line and error bars, mean +/- SEM. Statistical comparisons, Students t-test (unpaired, two-tailed); ****, p≤0.0001. Scale bar, 10 µm (C,D). dpw, days post wounding.
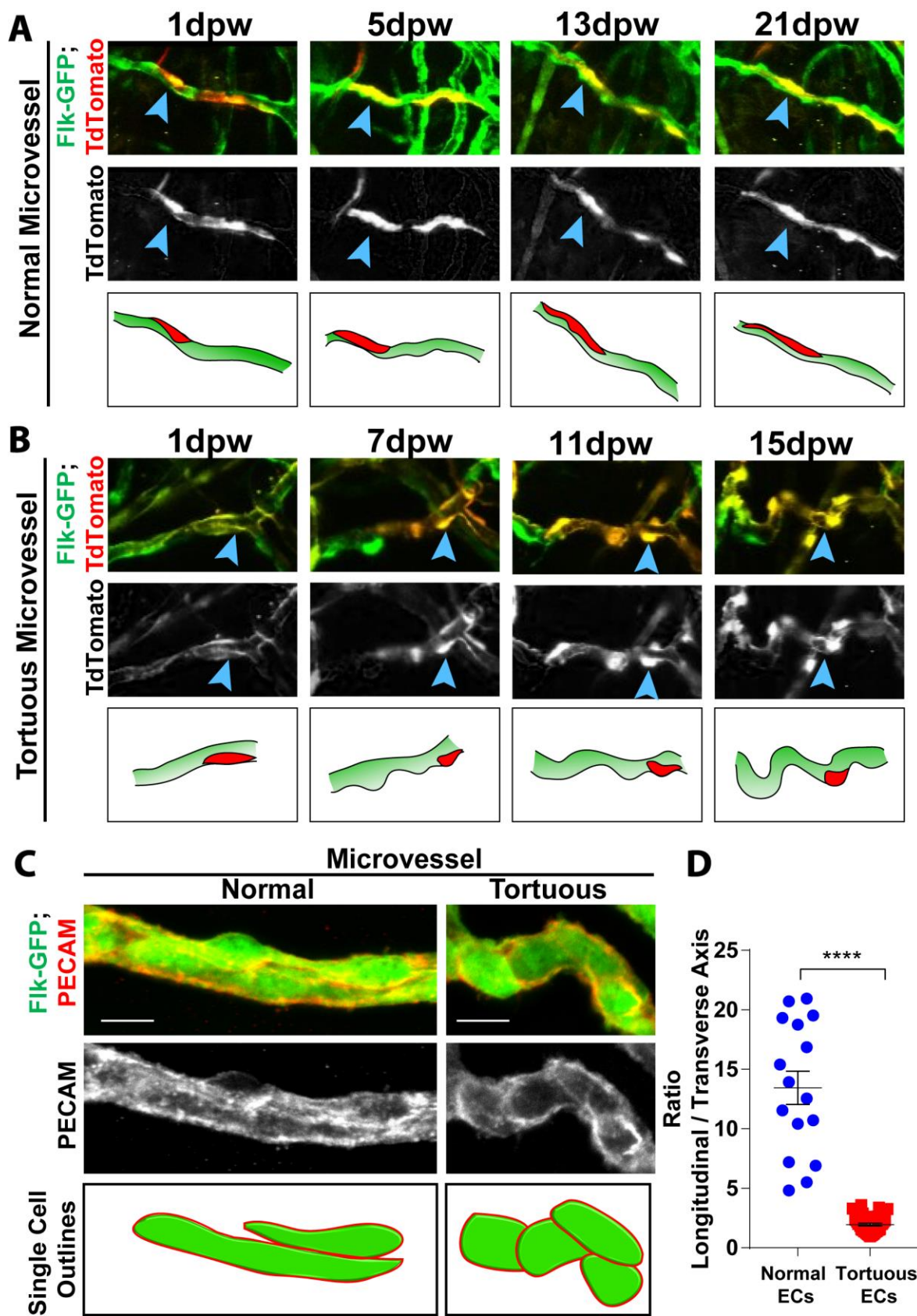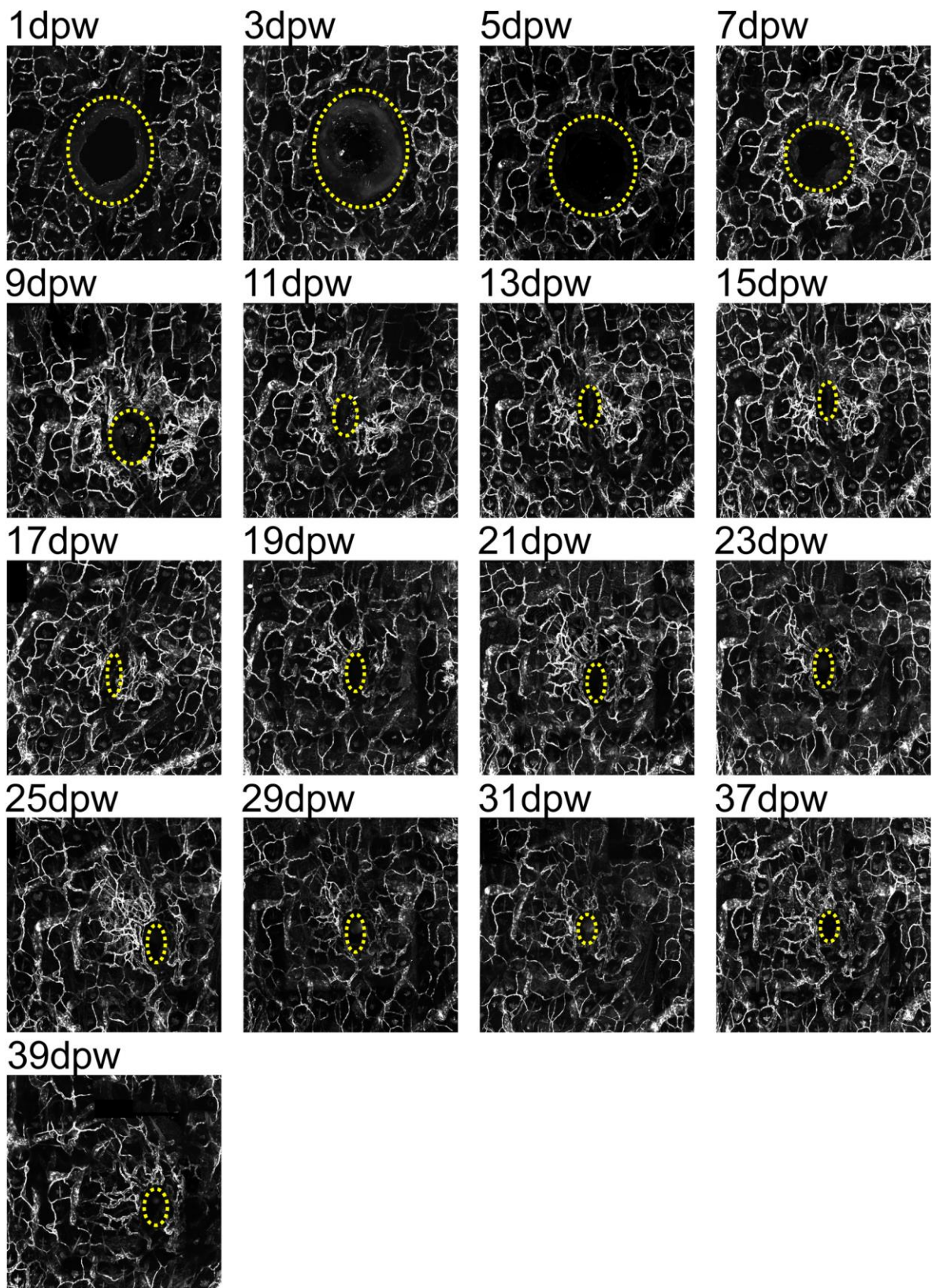
Figure 3.5. Tortuous microvessels have increased sprouting.

(A-F) Example of a normal microvessel near wound that became tortuous and initiated sprouting. (A) Normal microvessel near wound at 1dpw. (B) At 5dpw, the main microvessel became tortuous and initiated sprouting (blue arrows) from the apex of curved regions (yellow arrowheads). (C) Main microvessel remained tortuous and sprouts persisted at 7dpw. (D-F) From 9-15dpw, the main tortuous microvessel was normalized and the sprouts formed new connections (green arrows). (G) Quantification of sprout initiations from normal and tortuous microvessels during wound healing, n=3 ears. Error bars, mean $\pm$ SEM; Statistical comparisons: Two Way ANOVA with Sidak's Multiple Comparisons Test. *, $p \leq 0.05$; **, $p \leq 0.005$; ****, $p \leq 0.0005$. (H-K) Example of sprout initiation after tortuous microvessel formation. Note that sprout initiation does not occur until 9dpw (K, yellow arrow). (L) Quantification of sprout initiations subsequent to tortuous microvessel formation relative to sprout initiations simultaneous with tortuous microvessel formation. Error bars, mean $\pm$ SEM; Statistical comparisons: Students t-test (unpaired, two-tailed); **, $p \leq 0.005$. (M) Example of sprout initiation from apex of curve on tortuous microvessel. (N) Example of sprout initiation from non-curved region of tortuous microvessel. (O) Quantification of sprout initiations from the apex of tortuous microvessels relative to non-curved regions. Error bars, mean $\pm$ SEM; Statistical comparisons: Students t-test (unpaired, two-tailed); **, $p \leq 0.005$. (P) Model of tortuous microvessel initiation, sprouting, and resolution during wound healing. Scale bar, 50 µm (A). Vessels pseudo colored using Photoshop. dpw, days post wounding.
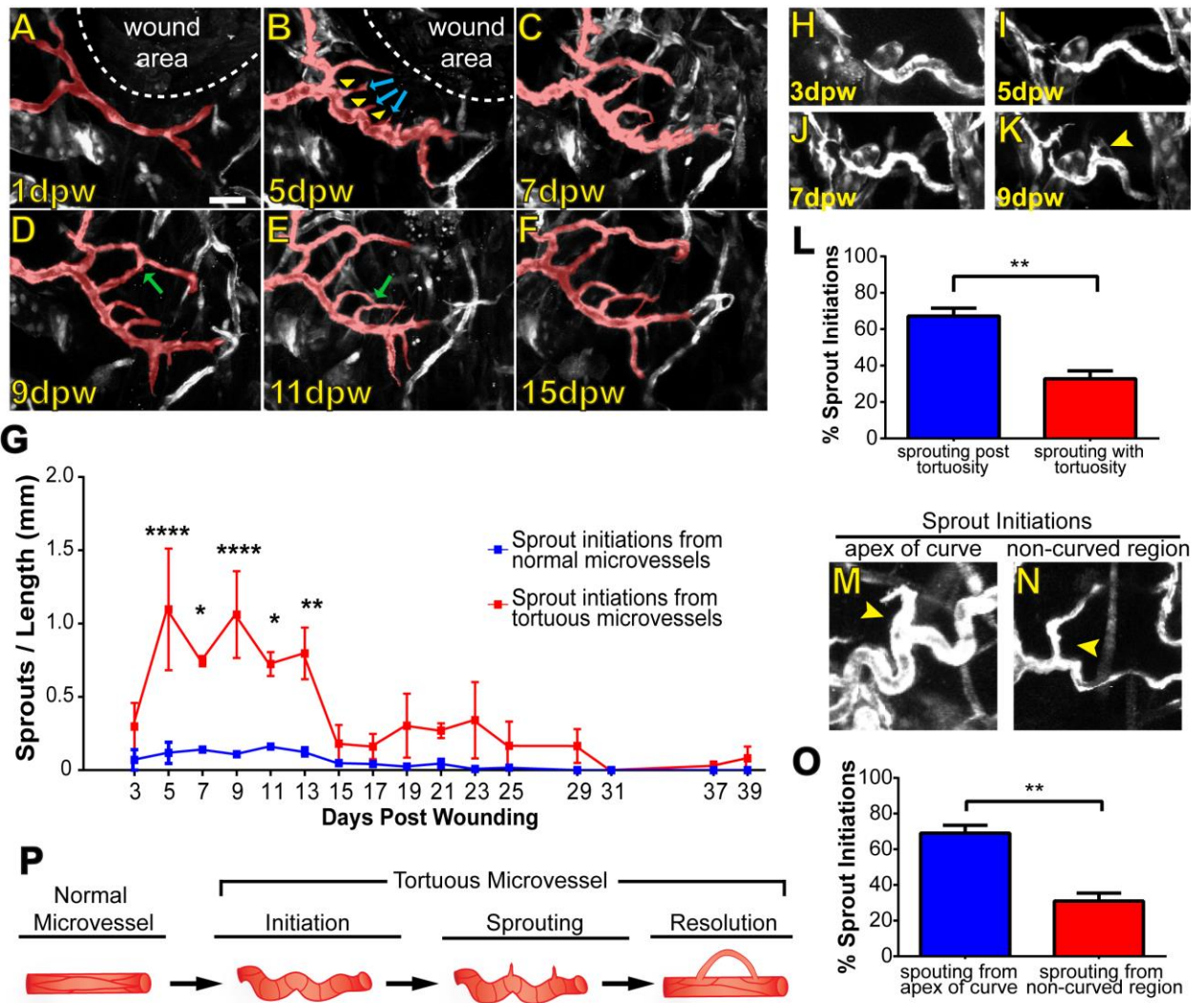
Supplementary Figure 3.1. Time course for wound healing in mouse ear.

Wound incurred at 0dpw. Z-stack image frames of wound area expressing Flk-GFP

(vascular, white) were stitched together for each time point and used for analysis. Yellow

stippled line, avascular area + punch wound at each time point. dpw, days post wounding.

1dpw 3dpw 5dpw 7dpw

9dpw 11dpw 13dpw 15dpw

17dpw 19dpw 21dpw 23dpw

25dpw 29dpw 31dpw 37dpw

39dpw

Supplementary Figure 3.2. Tortuosity index.

(A-B) Example of a normal microvessel segment (A) or tortuous microvessel segment (B), highlighting the geodesic distance (L_G, pink line), the Euclidean distance (L_E, blue line) and the number of inflection points (yellow stars). Note increased number of inflection points in tortuous vs. normal microvessel segment. On top is the equation used to calculate the tortuosity index (TI). (C) Quantification of TI values for normal and tortuous microvessel segments. Line and error bars, mean +/- SEM. Statistical comparisons: Students t-test (unpaired, two-tailed); ****, $p \leq 0.0001$. (D) Quantification of total microvessel length (normal and tortuous combined) over time. Error bars, mean $\pm$ SEM; *, $p \leq 0.05$; **, $p \leq 0.005$.

$$TI = L_G / L_E \times N_C$$
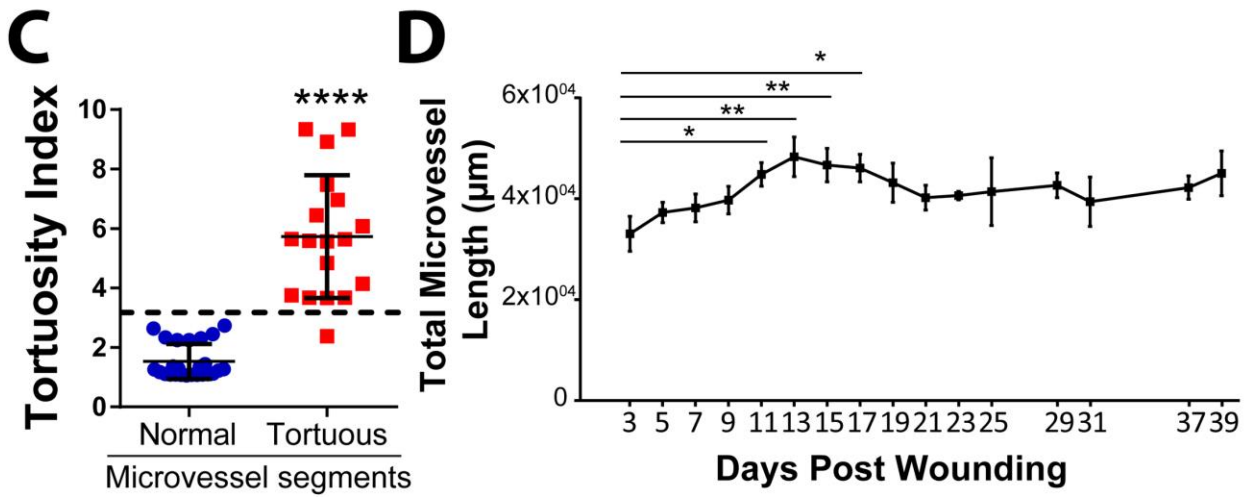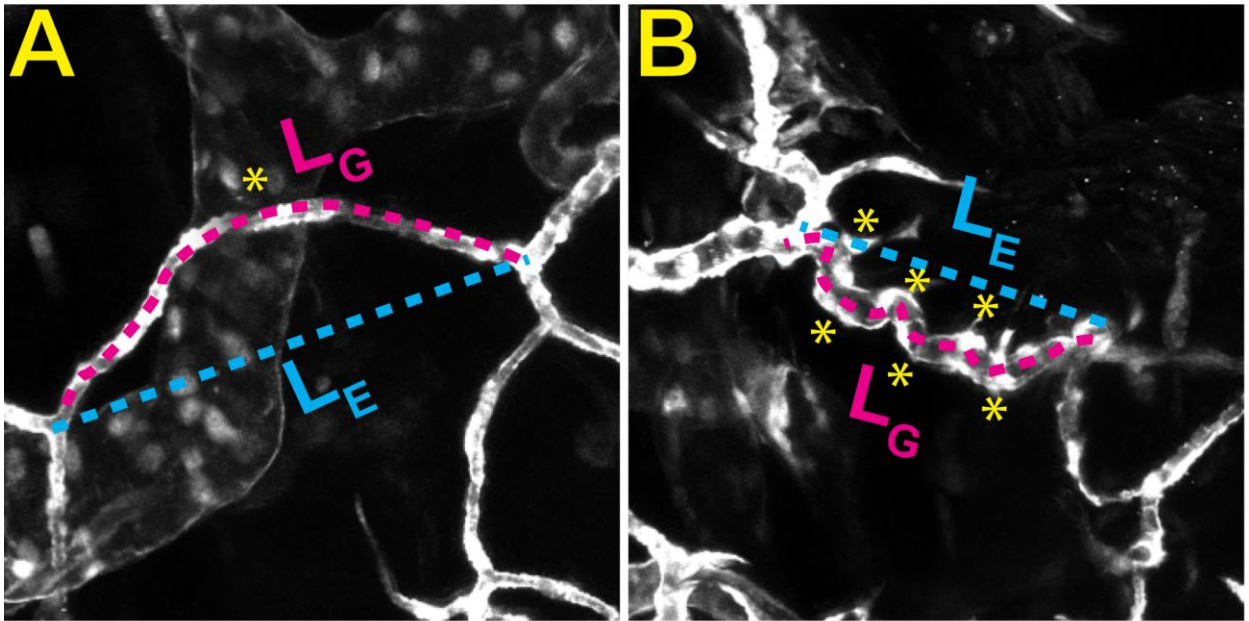
Supplementary Figure 3.3. The avascular area of the wound.

(A) Avascular area + wound punch outlined at 1dpw and used to analyze subsequent time points. (B) Defined 1 dpw area at subsequent time points. Segments pseudo colored with Photoshop to highlight the same region in each image. dpw, days post wounding.

A

1dpw
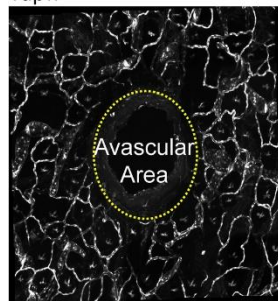
Avascular Area

B Defined avascular area from 1dpw outlined at subsequent timepoints

3dpw 5dpw 7dpw 9dpw 11dpw 13dpw 15dpw 17dpw

19dpw 21dpw 23dpw 25dpw 29dpw 31dpw 37dpw 39dpw
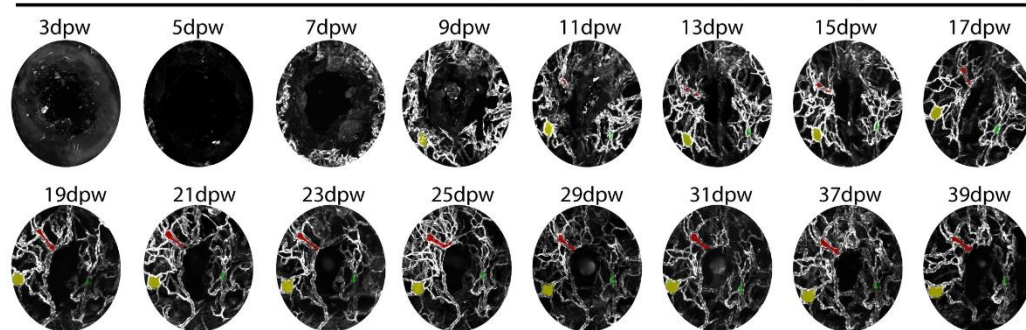
Supplementary Figure 3.4. Comparison of sprout dynamics.

(A) Example of sprout initiation from a tortuous microvessel (yellow arrow) that connected to another vessel segment (blue vessel). (B) Example of a sprout initiation from a tortuous microvessel (yellow arrow) that retracted. (C) Percentage of sprout initiations from normal (blue) or tortuous (red) microvessels that resulted in connections or retractions. (D) Percentage of tortuous microvessels that exhibited sprouting and normalized (blue), exhibited sprouting and did not normalize (red), or normalized absent sprouting (yellow). Vessels pseudo colored using Photoshop. dpw, days post wounding. Error bars, mean $\pm$ SEM; NS, not significant.
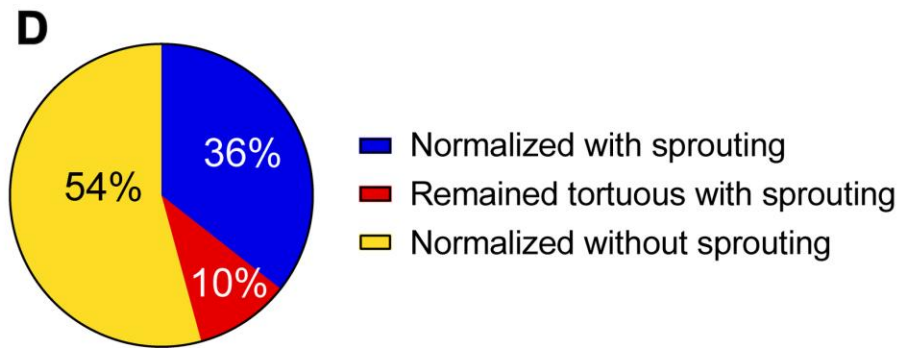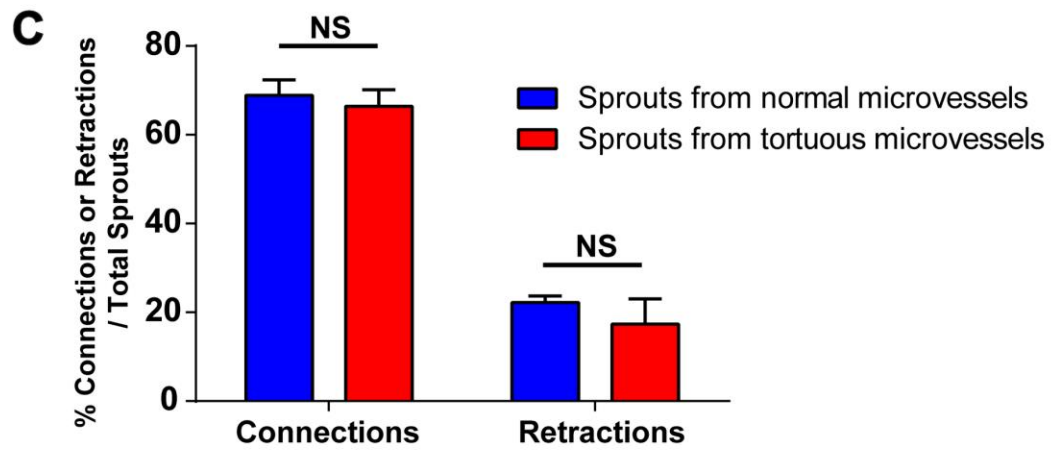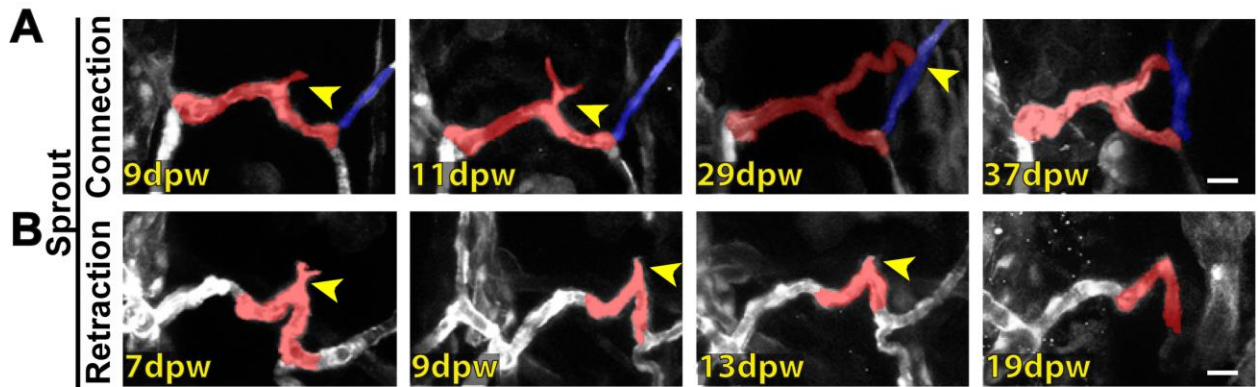
REFERENCES

1.   Adams RH, Alitalo K. Molecular regulation of angiogenesis and lymphangiogenesis. Nat Rev Mol Cell Biol. 2007;8(6):464-478.

2.   Chappell JC, Wiley DM, Bautch VL. How Blood Vessel Networks Are Made and Measured. Cells Tissues Organs 2011;195(1-2):94-107.

3.   Herbert SP, Stainier DYR. Molecular control of endothelial cell behaviour during blood vessel morphogenesis. Nat Rev Mol Cell Biol. 2011;12(9):551-564.

4.   Folkman J. Angiogenesis. Annu Rev Med. 2006;57:1-18.

5.   Risau W. Mechanisms of angiogenesis. Nature. 1997;386(6626):671-674.

6.   Chung AS, Ferrara N. Developmental and pathological angiogenesis. Annu Rev Cell Dev Biol. 2011;27:563-584.

7.   Kushner EJ, Bautch VL. Building blood vessels in development and disease. Curr Opin Hematol. 2013;20(3):231-236.

8.   Dvorak HF. Tumors: Wounds that do not heal--Redux. Cancer Immunol Res. 2015;3(1):1-11.

9.   Nagy JA, Chang SH, Dvorak AM, Dvorak HF. Why are tumour blood vessels abnormal and why is it important to know? Br J Cancer. 2009;100(6):865-869.

10.   Helisch A, Schaper W. Arteriogenesis The Development and Growth of Collateral Arteries. Microcirculation. 2003;10(1):83-97.

11.   Jain RK. Normalizing tumor vasculature with anti-angiogenic therapy: A new paradigm for combination therapy. Nat Med. 2001;7(9):987-989.

12.   Taarnhøj NCBB, Munch IC, Sander B, Kessel L, Hougaard JL, Kyvik K, et al. Straight versus tortuous retinal arteries in relation to blood pressure and genetics. Br J Ophthalmol. 2008;92(8):1055-1060.

13.   Han H-C. Twisted Blood Vessels: Symptoms, Etiology and Biomechanical Mechanisms. J Vasc Res. 2012;49(3):185-197.

14.   Greaves NS, Ashcroft KJ, Baguneid M, Bayat A. Current understanding of molecular and cellular mechanisms in fibroplasia and angiogenesis during acute wound healing. J Dermatol Sci. 2013;72(3):206-217.

15.   Wong VW, Crawford JD. Vasculogenic Cytokines in Wound Healing. Biomed Res Int. 2013;2013:11.

16. Singer AJ, Clark RAF. Cutaneous Wound Healing. N Engl J Med. 1999;341(10):738-746.

17. Rege A, Thakor NV, Rhie K, Pathak AP. In vivo laser speckle imaging reveals microvascular remodeling and hemodynamic changes during wound healing angiogenesis. Angiogenesis. 2012;15(1):87-98.

18. Hashizume H, Baluk P, Morikawa S, McLean JW, Thurston G, Roberge S, et al. Openings between Defective Endothelial Cells Explain Tumor Vessel Leakiness. Am J Pathol. 2000;156(4):1363-1380.

19. Jung Y, Dziennis S, Zhi Z, Reif R, Zheng Y, Wang RK. Tracking Dynamic Microvascular Changes during Healing after Complete Biopsy Punch on the Mouse Pinna Using Optical Microangiography. PLoS One. 2013;8(2):e57976.

20. Manning CS, Jenkins R, Hooper S, Gerhardt H, Marais R, Adams S, et al. Intravital imaging reveals conversion between distinct tumor vascular morphologies and localized vascular response to Sunitinib. IntraVital. 2013;2(1):e24790.

21. Ema M, Takahashi S, Rossant J. Deletion of the selection cassette, but not cis-acting elements, in targeted Flk1-lacZ allele reveals Flk1 expression in multipotent mesodermal progenitors. Blood. 2006;107(1):111-117.

22. Madisen L, Zwingman TA, Sunkin SM, Oh SW, Zariwala HA, Gu H, et al. A robust and high-throughput Cre reporting and characterization system for the whole mouse brain. Nat Neurosci. 2010;13(1):133-140.

23. Sörensen I, Adams RH, Gossler A. DLL1-mediated Notch activation regulates endothelial identity in mouse fetal arteries. Blood. 2009;113(22):5680-5688.

24. Chan KT, Jones SW, Brighton HE, Bo T, Cochran SD, Sharpless NE, et al. Intravital imaging of a spheroid-based orthotopic model of melanoma in the mouse ear skin. IntraVital. 2013;2(2):e25805.

25. Bullitt E, Gerig G, Pizer SM, Lin W, Aylward SR. Measuring Tortuosity of the Intracerebral Vasculature from MRA Images. IEEE Trans Med Imaging. 2003;22(9):1163-1171.

26. Kerber CW, Liepsch D. Flow dynamics for radiologists. II. Practical considerations in the live human. AJNR Am J Neuroradiol. 1994;15(6):1076-1086.

27. Saaristo A, Veikkola T, Enholm B, Hytönen M, Arola J, Pajusola K, et al. Adenoviral VEGF-C overexpression induces blood vessel enlargement, tortuosity, and leakiness but no sprouting angiogenesis in the skin or mucous membranes. FASEB J. 2002;16(9):1041-1049.

28.   Owen CG, Newsom RSB, Rudnicka AR, Barman SA, Woodward EG, Ellis TJ. Diabetes and the Tortuosity of Vessels of the Bulbar Conjunctiva. Ophthalmology. 2008;115(6):e27-e32.

29.   Eun Kim K, Cho C-H, Kim H-Z, Baluk P, McDonald DM, Young Koh G. In Vivo Actions of Angiopoietins on Quiescent and Remodeling Blood and Lymphatic Vessels in Mouse Airways and Skin. Arterioscler Thromb Vasc Biol. 2007;27(3):564-570.

30.   Ghaffari S, Leask RL, Jones EAV. Flow dynamics control the location of sprouting and direct elongation during developmental angiogenesis. Development. 2015;142(23):4151-4157.

31.   Lee S, Jilani SM, Nikolova GV, Carpizo D, Iruela-Arispe ML. Processing of VEGF-A by matrix metalloproteinases regulates bioavailability and vascular patterning in tumors. J Cell Biol. 2005;169(4):681-691.

32.   Brem H, Tomic-Canic M. Cellular and molecular basis of wound healing in diabetes. J Clin Invest. 2007;117(5):1219-1222.

33.   Tahergorabi Z, Khazaei M. Imbalance of Angiogenesis in Diabetic Complications: The Mechanisms. Int J Prev Med. 2012;3(12):827-838.

Chapter 4: General Discussion

4.1 Endothelial deletion of BMPR2 decreases sprouting during retinal development

BMP signaling increases sprouting angiogenesis and vascular branching in the developing retina. Here, we showed that BMP2,4,6,7 ligands are found in the retina from P1-P6 and that the BMP receptors, ALK1, ALK2, ALK3, and BMPR2 are enriched in blood vessels of the retina. Endothelial specific deletion of Bmpr2, Alk2, and Alk3 resulted in decreased sprouting at the vascular front and decreased branching in the plexus while deletion of Alk1 resulted in increased branching. These results indicate that BMP signaling is not required to initiate angiogenesis, but is required for expansion of the network and maintenance.

Previously, BMP signaling has been implicated as being a pro-angiogenic cue for ectopic sprouting from veins. Wiley et al. showed that overexpressing the *bmp2b* ligand in zebrafish resulted in increased sprouting from only the venous compartment [1]. Interestingly, we did not find that BMP expression or activity was restricted to veins in the postnatal mouse retina. We found that BMP receptors were pan-endothelial, suggesting that manipulating BMP signaling would not be restricted to a vessel type in this vascular bed. A recent study shows that the ability of endothelial cells to sprout in response to BMP is correlated to the level of Notch activity in individual cells [2]. When Notch activity is high, endothelial cells do not sprout in response to BMP overexpression. In zebrafish, Notch signaling is robust in the dorsal aorta, inhibiting cells from the aorta to be able to respond to

BMP. In contrast, Notch activity is low in the postnatal retina [3]. From P3-P5, Notch activity is present in sporadic cells and is not robustly present in the arteries over veins. Thus, since Notch activity is low in the retina, it is possible that Notch signaling is not a limiting factor in BMP responsiveness in the postnatal retina. This explains why we did not observe changes in sprouting frequency from specific vessel types; instead, sprouting was affected in all vessel types.

Although most BMP signaling components have been shown to be pro-angiogenic during development [4], the interaction between BMP9/BMP10 and receptor, Alk1, has been shown to have an anti-angiogenic role. Here, we found that endothelial specific deletion of the Alk1 receptor resulted in increased vascular density, consistent with an anti-angiogenic effect. However, of note is the fact that there is little BMP9 and BMP10 mRNA in the retina, so why is there an effect when Alk1 is knocked down? It has been reported that BMP9 and BMP10 ligands are mainly found in circulation and that the amounts of these ligands are higher during birth than in adulthood [5]. Thus, examining mRNA in the retina could be misrepresenting the physiological levels of BMP9/10 and their effect on angiogenesis. Since there was significantly increased vessel density with the endothelial specific knock-out of Alk1, we can predict that BMP9 and BMP10 are active in the retina, even if the ligands are not being produced in the retina.

We showed that the ALK3/BMPR2 signaling axis provides a stronger contribution to sprouting at the vascular front, compared to ALK2/BMPR2 which has a stronger effect on vascular branching behind the vascular front. The stronger effects of Alk3 on sprouting could be due to the presence of Alk3 on filopodia tips. Pi et al showed that ALK6 translocates to filopodial tips after BMP6 stimulation [6]. Since ALK3 and ALK6 share structural homology

(85% in their kinase domain and 42% in the extracellular domain) and BMP6 binds preferentially to ALK3 over ALK6 [7], it is possible that ALK3 is also present at the tips of filopodia and is aiding in sprout guidance. The presence of ALK3 at filopodia tips would explain the different phenotypes observed between endothelial specific deletion of *Alk2* and *Alk3*.

4.2 Tortuous vessels exhibit unique properties and increased sprouting angiogenesis

Tortuous vessels are abnormal vessels associated with wound healing and disease. The causes and consequences of tortuous vessels remain understudied. Here, we provided an in-depth analysis of tortuous microvessels during wound healing. We showed that tortuous vessels form through sprouting angiogenesis and resolve by becoming normal vessels. By imaging microbeads in circulation, we predict flow differences between normal and tortuous vessels, possibly leading to activation of endothelial cells within tortuous vessels and causing them to sprout robustly.

A question that remains unanswered is, why are tortuous vessels present in the wound in the first place? Our data shows that tortuous microvessels sprout at a higher frequency than normal vessels, increasing the vessel density near the wound. Previous reports have stated that the vessel density can be up to 10x the normal amount after a wound is made [8]. A mechanism in which vessels are able to grow and sprout rapidly is needed to account for the exponential growth, and tortuous microvessel formation and sprouting could be the answer to rapid expansion of the vascular network. Additionally, tortuous microvessels are leakier than normal vessels (data not shown), suggesting increased extravasation of solutes to the wound area, thereby increasing the rate of healing. Thus, the role of tortuous vessels near

the wound could be for rapid expansion of the vessel network allowing for increased solute and immune cell transport and secretion to the wound site.

One idea on how tortuous vessels form centers on the effect of changes to extracellular matrix on vessel morphology. Multiple studies, including genetic KO mouse models, have shown that providing an unsupportive matrix environment can lead to tortuosity [9]. When surrounding connective tissue degrades or is not stiff enough to support the vessel, tortuosity can occur [10]. Mice lacking the elastin component, FIBULIN5, developed tortuous arteries due to decreased elastic fibers that cannot fully support arteries [11]. Additionally, continuously stretching rat ears by applying a constant tensile force can change the viscoelastic properties, stimulating cell proliferation and vessel remodeling, ultimately resulting in tortuous vessels [12]. Skin stretching elevated expression of HIF-1α and VEGF, but had minimal effects on the inflammatory response. Taken together, this data suggests that the tortuous microvessels I observed during wound healing can be attributed to changes in the ECM associated with wound healing. Although I am able to visualize collagen I fibers using second harmonics generated by two-photon excitation [13], I did not observe any obvious changes in collagen deposition during wound healing. In fact, the collagen matrix was behind the leading vascular front, where most tortuous microvessels are formed. However, this does not rule out the possibility of other matrix components contributing to tortuous microvessel formation, such as collagen IV. Collagen IV is a basement membrane component that significantly contributes to vessel elongation, proliferation, and stabilization, [14], thus it would be of interest to analyze this particular ECM component during wound healing.

We observed that tortuosity "activates" endothelial cells and is upstream of sprout initiations. Even though multiphoton intravital imaging has been around for a few decades [15], sprouting from tortuous vessels has not been previously documented, to our knowledge. Yet, one intravital imaging study that focused on the tumor microvasculature noted the presence of tortuous vessels and sprouting [16]. Manning et al. found that vascular margins existed around a tumor with varying degrees of vessel tortuosity. Although they showed one example of a sprouting event near the tumor, they noted that the tortuous vessel became linear before the sprout was observed. Considering tumors and wounds have similar microenvironments [17], it is surprising that the authors did not observe sprouting from tortuous microvessels. One explanation for this inconsistency is that the authors were not actively looking for sprouting events and could have missed sprout initiations from tortuous vessels. Yet another explanation is that a vascular front does not exist in tumor angiogenesis, so it may be difficult to visualize sprout initiations at the same capacity as wound healing, where the vascular front encapsulates the wounded tissue.

My studies have uncovered a new characteristic of tortuosity, sprouting, that can be used as a target for tortuous vessel normalization or anti-angiogenic therapies. Understanding the differences between normal and tortuous vessels and how tortuous vessels form and resolve during wound healing are key to unlocking mechanisms to combat cancer.

4.3 Tortuous vessel normalization to combat disease

Tortuous vessels are observed in many diseases, ranging from cancer and diabetes to atherosclerosis and hypertension [10]. Even though tortuous vessels can be used as a prognostic marker for these diseases, the outcome on vessel density can vary. For example,

the tumor environment promotes vessel growth whereas diabetes promotes ischemia and inhibits vascular growth. Therefore, careful consideration for the disease mechanisms and their impact on angiogenesis must be taken when trying to find a suitable therapy.

Studies pioneered by Dr. Judah Folkman revealed that angiogenesis is a major contributor of tumor growth and that tumors secrete factors that attract blood vessels [18]. Since his initial observations almost 50 years ago, cancer therapies are still aimed at targeting the tumor microvasculature to inhibit tumor growth and metastasis. Mostly, anti-angiogenic therapies have been used in conjunction with chemotherapy to decrease proliferating endothelial cells [19, 20], however this treatment has not been completely effective and the endothelial cells that escape and repopulate the tumor environment become resistant to anti-angiogenic drugs and exhibit increased virulence [21, 22]. More recently, a new concept has emerged that focuses on normalizing the tortuous vessels in the tumor microenvironment, i.e. making the vessels less leaky, to increase the efficiency of cancer drugs reaching their target [23]. Normalizing abnormal tumor vessels in a breast cancer mouse model enhanced the efficacy of an anticancer vaccine therapy [24], providing credibility to this new hypothesis. Since tortuous vessels naturally resolve after a wound is healed, the mechanisms that lead to abnormal vessel normalization can be deciphered from further in depth studies of tortuous microvessels and wound healing. Finding biomarkers that distinguish normal and tortuous vessels would be ideal in performing RNA-seq between the two different endothelial populations during the different phases of wound healing. The results from this experiment could unravel the important mechanisms involved in tortuous vessel resolution. Based on my studies and the literature, I predict that genes that are upregulated during inflammation, such

as *Vcam-1* and *Icam-1*, are also increased in tortuous endothelial cells. Thus, reducing the inflammatory response may be a key factor in tumor vessel normalization.

Not all tortuous vessels share the same properties. Collateral vessels are small vessels that do not experience flow under normal circumstances. In the event of an arterial occlusion, the surrounding collateral arteries are used to bypass the occlusion and maintain proper circulation [25]. It is not known whether collateral tortuosity is present before flow and predetermined by spatial restrictions or whether the onset of flow in collaterals induces tortuosity. However, since the main function of these arteries is to maintain flow, permeability in these vessels would not be favorable. A comparison between tortuous collateral arteries and wound-associated tortuous microvessels would reveal additional mechanisms that regulate permeability. In the tumor microenvironment, leaky tortuous vessels do not allow efficient drug penetration to the tumor [26]. Therefore, making tortuous vessels less permeable would increase dose delivery of anti-cancer drugs to the tumor, making current cancer therapies more effective.

I have argued that increased angiogenesis during wound healing is advantageous, however excessive angiogenesis can lead to increased scarring [8, 27]. In fetal and oral mucosa wounds, there is a decreased inflammatory response and angiogenesis, resulting in reduced scar formation [28, 29]. One idea is that apoptosis of endothelial cells during the remodeling phase contributes to the scar tissue [8]. Anti-angiogenic drugs applied to wounds lead to normal wound closure suggesting that the angiogenic response during wound healing is excessive, unnecessary, and increases scarring. Thus, since tortuous microvessels sprout robustly and increase vessel density near the wound, normalizing tortuosity during wound healing can decrease angiogenesis and vessel density, leading to decreased scarring.

Although this would be beneficial from a cosmetic point of view, it is important to keep in mind that not all wounds have excessive angiogenesis. Diabetic wounds have decreased vascularization and ischemia, therefore treating diabetic wounds with anti-angiogenic drugs would not be recommended.

4.4 Summary

In conclusion, I have emphasized the importance of BMP signaling during developmental angiogenesis and highlighted the complexities of the signaling pathway. Additional genetic manipulation of the different ligands and receptors will further elucidate any additional roles BMP has on angiogenesis. I have also provided an in-depth discussion of tortuous vessels and how they can be used as a therapeutic target. Further studies into the direct mechanisms that cause and resolve tortuosity will be vital in vessel normalization strategies.

REFERENCES

1.   Wiley DM, Kim J-D, Hao J, Hong CC, Bautch VL, Jin S-W. Distinct Signaling Pathways Regulate Sprouting Angiogenesis from the Dorsal Aorta and Axial Vein. Nature cell biology. 2011;13(6):686-692.

2.   Mouillesseaux KP, Wiley DS, Saunders LM, Wylie LA, Kushner EJ, Chong DC, et al. Notch regulates BMP responsiveness and lateral branching in vessel networks via SMAD6. Nature Communications. 2016;7:13247.

3.   Hofmann JJ, Iruela-Arispe ML. Notch Expression Patterns in the Retina: An Eye on Receptor-Ligand Distribution during Angiogenesis. Gene expression patterns : GEP. 2007;7(4):461-470.

4.   Dyer LA, Pi X, Patterson C. The role of BMPs in endothelial cell function and dysfunction. Trends in endocrinology and metabolism: TEM. 2014;25(9):472-480.

5.   Ricard N, Ciais D, Levet S, Subileau M, Mallet C, Zimmers TA, et al. BMP9 and BMP10 are critical for postnatal retinal vascular remodeling. Blood. 2012;119(25):6162-6171.

6.   Pi X, Ren R, Kelley R, Zhang C, Moser M, Bohil AB, et al. Sequential roles for myosin-X in BMP6-dependent filopodial extension, migration, and activation of BMP receptors. The Journal of Cell Biology. 2007;179(7):1569-1582.

7.   Lee NY, Kirkbride KC, Sheu RD, Blobe GC. The Transforming Growth Factor-β Type III Receptor Mediates Distinct Subcellular Trafficking and Downstream Signaling of Activin-like Kinase (ALK)3 and ALK6 Receptors. Molecular Biology of the Cell. 2009;20(20):4362-4370.

8.   DiPietro LA. Angiogenesis and wound repair: when enough is enough. Journal of Leukocyte Biology. 2016;100(5):979-984.

9.   Han H-C. Blood vessel buckling within soft surrounding tissue generates tortuosity. Journal of Biomechanics. 42(16):2797-2801.

10.   Han H-C. Twisted Blood Vessels: Symptoms, Etiology and Biomechanical Mechanisms. Journal of Vascular Research. 2012;49(3):185-197.

11.   Nakamura T, Lozano PR, Ikeda Y, Iwanaga Y, Hinek A, Minamisawa S, et al. Fibulin-5/DANCE is essential for elastogenesis in vivo. Nature. 2002;415(6868):171-175.

12.   Pietramaggiori G, Liu P, Scherer SS, Kaipainen A, Prsa MJ, Mayer H, et al. Tensile Forces Stimulate Vascular Remodeling and Epidermal Cell Proliferation in Living Skin. Annals of Surgery. 2007;246(5):896-902.

13. Chen X, Nadiarynkh O, Plotnikov S, Campagnola PJ. Second harmonic generation microscopy for quantitative analysis of collagen fibrillar structure. Nature protocols. 2012;7(4):654-669.

14. Bonanno E, Iurlaro M, Madri JA, Nicosia RF. Type IV collagen modulates angiogenesis and neovessel survival in the rat aorta model. In Vitro Cell Dev Biol Anim. 2000;36(5):336-340.

15. Weigert R, Porat-Shliom N, Amornphimoltham P. Imaging cell biology in live animals: Ready for prime time. The Journal of Cell Biology. 2013;201(7):969-979.

16. Manning CS, Jenkins R, Hooper S, Gerhardt H, Marais R, Adams S, et al. Intravital imaging reveals conversion between distinct tumor vascular morphologies and localized vascular response to Sunitinib. IntraVital. 2013;2(1):e24790.

17. Dvorak HF. Tumors: wounds that do not heal. Similarities between tumor stroma generation and wound healing. N Engl J Med. 1986;315(26):1650-1659.

18. Folkman J. Tumor Angiogenesis: Therapeutic Implications. New England Journal of Medicine. 1971;285(21):1182-1186.

19. Nishida N, Yano H, Nishida T, Kamura T, Kojiro M. Angiogenesis in Cancer. Vascular Health and Risk Management. 2006;2(3):213-219.

20. Hurwitz H, Fehrenbacher L, Novotny W, Cartwright T, Hainsworth J, Heim W, et al. Bevacizumab plus Irinotecan, Fluorouracil, and Leucovorin for Metastatic Colorectal Cancer. New England Journal of Medicine. 2004;350(23):2335-2342.

21. Weis SM, Cheresh DA. Tumor angiogenesis: molecular pathways and therapeutic targets. Nature Medicine. 2011;17:1359+.

22. Bergers G, Hanahan D. Modes of resistance to anti-angiogenic therapy. Nat Rev Cancer. 2008;8(8):592-603.

23. Goel S, Wong AH-K, Jain RK. Vascular Normalization as a Therapeutic Strategy for Malignant and Nonmalignant Disease. Cold Spring Harbor Perspectives in Medicine. 2012;2(3):a006486.

24. Huang Y, Yuan J, Righi E, Kamoun WS, Ancukiewicz M, Nezivar J, et al. Vascular normalizing doses of antiangiogenic treatment reprogram the immunosuppressive tumor microenvironment and enhance immunotherapy. Proceedings of the National Academy of Sciences of the United States of America. 2012;109(43):17561-17566.

25. Schaper W, Scholz D. Factors Regulating Arteriogenesis. Arteriosclerosis, Thrombosis, and Vascular Biology. 2003;23(7):1143-1151.

26.   Hashizume H, Baluk P, Morikawa S, McLean JW, Thurston G, Roberge S, et al. Openings between Defective Endothelial Cells Explain Tumor Vessel Leakiness. The American Journal of Pathology. 2000;156(4):1363-1380.

27.   Singer AJ, Clark RAF. Cutaneous Wound Healing. New England Journal of Medicine. 1999;341(10):738-746.

28.   Szpaderska AM, Zuckerman JD, DiPietro LA. Differential Injury Responses in Oral Mucosal and Cutaneous Wounds. Journal of Dental Research. 2003;82(8):621-626.

29.   Leung A, Crombleholme TM, Keswani SG. Fetal wound healing: implications for minimal scar formation. Current opinion in pediatrics. 2012;24(3):371-378.